ULTRA-PRECISION MACHINING OF ELECTROLESS-NICKEL PLATED DIE MATERIAL

ALOKESH PRAMANIK

(B. Sc in MECHANICAL ENGINEERING)

A THESIS SUBMITTED

FOR THE DEGREE OF MASTER OF ENGINEERING

DEPARTMENT OF MECHANICAL ENGINEERING

NATIONAL UNIVERSITY OF SINGAPORE

2004

ACKNOWLEDGMENT

The author wishes to express his sincerest gratitude and indebtedness to Dr. Mustafizur Rahman, Associate Professor of the Department of Mechanical Engineering, National University of Singapore, for his guidance, supervision and moral support throughout the entire period of research work. His initiative, encouragement, patience and valuable suggestions are gratefully acknowledged.

The author wishes to express thanks and regards to Dr. Li Xiaoping, Associate Professor of the Department of Mechanical Engineering, National University of Singapore, for his guidance, supervision and valuable advice to complete the work successfully.

Special thanks are offered to Mr. Neo Ken Soon, Professional officer, AML, National University of Singapore, for his all kinds of technical support and suggestion. Many thanks to Mohamed Noh Bin Mohamed Kasim, final year student, National university of Singapore, for helping in collection and calculation of some experimental data.

The author also extends his gratitude equally to all staff of Advance Manufacturing Lab especially to Mr. Tan Choon Huat and Mr. Nelson Yeo for their cooperation and assistance at different stages of research work.

The final expression of gratitude is offered to all professors and staff of the Mechanical Engineering Department, National University of Singapore for their assistance and valuable advice.

TABLE OF CONTENTS

SUMMARY

Study on ultra-precision machining has increased since the 1960s and now it is relatively mature technology by which a submicron tolerance and a nanometer surface finish can be achieved. The most popular metals in optical field for ultra-precision machining, namely copper and aluminum, offer surfaces that can easily be ruined by abrasion and corrosion from cleaning and handling in molding applications. Most of the materials are not suitable for diamond turning. A very useful metal in these fields is nickel-phosphorus alloy, chemically deposited from an aqueous solution and commonly known as “electroless nickel” which is hard, corrosion resistant, have a wide range of properties with the change of phosphorus content. Best of all, diamond machines electroless nickel very well. Although there is research in the machining of electroless nickel, information regarding the relationship between the surface roughness and cutting forces, and the machining parameters cannot found. Moreover there is no research record of cutting electroless nickel with different phosphorus content for very long cutting distances by any type of diamond tool.

This study is an attempt (a) to optimize various cutting parameters such as depth of cut, feed rate, spindle speed and phosphorus content, (b) to observe and compare the performance of two types of diamond tools (natural and artificial) for a long cutting distance (200 km), (c) to study the effects of wear on the surface roughness and cutting forces, and (d) to investigate the effect of depth-of-cut on artificial diamond cutter for very long cutting distances.

The experimental results show that higher feedrate gives worse surface finish and higher cutting forces, however with the increase in phosphorus content, the surface

finish becomes better and cutting forces decrease. It appears that depth-of-cut does not have any significant effect on surface roughness but cutting forces increase with the increase of depth-of-cut. In case of increasing spindle speed, cutting forces increase slightly, and for the best surface there is a critical value of spindle speed. During testing of performance of natural and artificial diamond cutters, it was found that natural diamond cutters performed better than that of artificial diamond in terms of wear, surface finish and forces, although the cost of natural diamond cutter was three to four times higher than that of artificial diamond cutter. When electroless nickel with different phosphorus content was machined, severe tool wear was observed for lower phosphorus contents, but tool wear was negligible for higher phosphorus contents. Very good surface finish was achieved for higher phosphorus contents. In machining long cutting distances the lower depth-of-cut gave higher tool wear although the performances in other fields, i.e surface finish and forces, were nearly the same as for higher depth-of-cut.

NOMENCLATURE

τ_i = the resistance of the lattice to dislocation movement

k'= a parameter related to release of dislocations from a pile-up

γ_s= the effective surface energy including the energy of plastic deformation

β = a term which expresses the ratio of shear stress to normal stress. For torsion 1; for tension ½; for notch $^1/_3$

D = diameter of grain

G = modulus of rigidity

σ_0 = the yield stress

σi = the "friction stress" representing the overall resistance of the crystal lattice to dislocation movement.

k = the "locking parameter" which measures the relative hardening contribution of the grain boundary

θe = temperature in chip formation zone

θ_0 = initial workpiece temperature

Γ = proportion of heat conducted from chip formation zone to workpiece

A = cutting edge temperature rise factor amplitude

F_c = cutting force in cutting direction

F_f = friction force on tool face

r_c = ratio of undeformed chip thickness to deformed chipthickness

a_c = undeformed chip thickness

a_w = width of cut

ρ = workpiece density

c = workpiece specific heat capacity

H = hardness

α = non dimensional constant related to poisson's ratio

Φ = constraint factor ≈ 3

E = Young's Modulus

ν = Poisson's ratio

K_{IC} = critical stress intensity factor or fracture toughness

c = crack length

a= half of the average of two diagonals of the indentation mark

a_{cmin} = minimum undeformed chip thickness

ρ = cutting edge radius of cutting tool

F_t = thrust force

F_c = cutting force

μ = coefficient of friction

d_c = the critical undeformed chip thickness or the critical indentation depth

H = material hardness

R = material's fracture energy

u = brittle-ductile transition factor of the material

K_c= fracture toughness

LIST OF FIGURES

LIST OF PAPERS PUBLISHED

Publication in Journal:

1. A. Pramanik, K.S. Neo, M. Rahman, X. P. Li, M. Sawa, Y. Maeda, "Cutting performance of diamond tools during ultra-precision turning of electroless nickel plated die materials", Volume 140, Issues 1-3 , 22 September 2003, Pages 308-313, Journal of Materials Processing Technology, Elsevier Science.

Publications in conference:

1. A. Pramanik, K.S. Neo, M. Rahman, X. P. Li, M. Sawa, Y. Maeda, "Comparison of cutting performance of artificial and natural diamond tools during ultra-precision machining of electroless nickel plated die materials", International conference on precision engineering 2003/04 (IcoPE2003/04), 2-5 March 2004, Singapore (accepted).

2. A. Pramanik, K.S. Neo, M. Rahman, X. P. Li, M. Sawa, Y. Maeda, " Ductile cutting of Brittle Materials", International Conference on Materials for Advanceed Technologies (ICMAT-2003), December 7-12, 2003, Singapore. (Accepted- not published).

3. Alokesh Pramanik, Neo ken Soon, M. Rahman, X. P. Li, M. Sawa, Y. Maeda, "Effect of machining conditions and phosphorus content in nano-precision machining of electroless nickel", First Humanoid, Nanotechnology, Information Technology, Communication and Control Environment and Management (HNICEM) International Conference March 27-30, 2003,p-49 Manila, Philippines.

4. Alokesh Pramanik, Neo ken Soon, M. Rahman, M. Sawa, Y. Maeda, "Ultra-precision machining of electroless nickel plated die materials". Proceedings of the International Conference on Manufacturing (ICM-2002), Vol-1 pp180-185, August 09-11 2002, Dhaka, Bangladesh.

1

INTRODUCTION

1.1 AN OVERVIEW

The modern age can be called the age of nanotechnology. “Nanotechnology” is the term used to indicate the integrated manufacturing technologies and machining system, which provide ultra-precision machining capability in the order of 1 nanometer (0.001μm = 1nm). Nanotechnology, perhaps today’s most advanced manufacturing technology, might also be called the “extreme technology” because the theoretical limit of accuracy in machining of substance must be the size of an atom or molecule of the substance (0.2nm to 0.4nm). The thin film technology required for the next generations of semi-conductors demands to study of ‘extreme technology’ problems and techniques; individual atoms have to be controlled and positioned where required. In this sense ultra-precision machining technology is already approaching the extreme of ultimate limits [1].

The miniaturization of mechanical, fluidic, biotechnological and optical component is still in its early stage [2]. As new areas of application for these components are explored, this leads to new requirements that cannot be met with current manufacturing technology. Only nano-technology can satisfy these requirements with ultra-precision machining. Research in micro machining has been reported since the late sixties. These activities resulted in what is very well known as ultra-precision machining. The primary goal of ultra precision machining is to achieve an optical surface roughness of a few nanometers RMS by using single crystal diamond tool [3].

For ultra-precision machining there is no alternative of using diamond-cutting tool on an ultra-precision lathe under very precisely controlled machining and environmental conditions to fabricate components. Diamond turning started before 1944 but diamond for optics was used in 1960's but did not start to gain recognition until the mid 1970's. Around that time electroplated and electroless-nickel plated coating started to be used as workpiece as these coatings offer significant materials flexibility for machined optics as well as providing high reflective surface [4]. In the very beginning precision machining technology was new and no systematic work was available to determine which coating are diamond turnable and which are not, nor had mechanism to explain why one coating is turnable and another is not [4]. Day by day the importance of electroless-nickel coating was recognized and study of ultra-precision machining of electroless-nickel plate started. The most popular metal in optical field for diamond machining, namely copper and aluminum, offer surface that can easily be ruined by abrasion and corrosion from cleaning and handling, also in molding applications, most of the materials are not suited for diamond turning. In this instance very useful metals in these fields are nickel-phosphorus alloys, chemically deposited from an aqueous solution and commonly known as "electroless nickel" which is hard, corrosion resistant. They have wide range of properties with the change of phosphorus content and, best of all, diamond machines electroless nickel very well [5]. Even with these important facts there is no complete work on machining of electroless-nickel and wear behavior of diamond tool in cutting of electroless-nickel for long distance. The objectives of this investigation are briefly described in the following.

1.2 OBJECTIVES

a. To find out the effects of cutting parameter in ultra-precision machining of electroless-nickel in terms of surface roughness, surface appearance, cutting forces and cutting tool wear. Here the input cutting parameters were depth of cut, feed rate and spindle speed.
b. To observe the cutting performance of cutting tools for very long cutting distance (>200km) in terms of surface roughness, surface appearance, cutting force and amount of tool wear.
c. To compare the cutting performance of artificial and natural diamond tools.
d. To compare the cutting tool performance in cutting electroless-nickel with different phosphorus content.
e. To develop the theory for brittle to ductile mode chip formation mechanism.

1.3 ORGANIZATION OF THESIS

A brief summary of relevant literature pertaining to electroless-nickel and its machining are discussed in chapter 2. Investigations on theoretical aspect of ductile cutting of brittle materials and factors for transition of brittle-to-ductile mode machining are discussed in chapter 3. Chapter 4 describes the experimental setup and procedure, the details about workpieces, cutting tools, machining parameters, surface measurement system, cutting forces data acquisition system and taking pictures of surfaces and cutting edges. The experimental results are analyzed in details in chapter-

5. The conclusions derived form this experimental works are summarized and a brief discussion on the future directions of the work is provided in chapter 6.

2

LITERATURE REVIEW

2.1 INTRODUCTION

Electroless-nickel plating provides a deposit that follows all contours of the substrate exactly, without building up at the edges and corners and achieves unique physical characteristics, including excellent corrosion, wear and abrasion resistance, ductility, lubricity, solderability, conductivity, high hardness and durability [6]. Electroless-nickel plating system is “auto-catalytic” (self-catalyting), meaning that it will continue to plate onto its own deposits after the substrate has been completely covered. It can be plated to substantial thickness. The deposits exhibit a good as-plated hardness and this can be controlled by heat treatments. Since deposits are uniform in thickness over all surfaces, irregular shapes can be plated by electroless-nickel [7].

As early as 1844, Wurtz discovered that metallic nickel could be deposited from the aqueous solution of its salts by reduction with hypophosphite. In the years that followed, the reaction was much studied (on test tube scale) but the metal thus formed was almost invariably in powder form. A handful of researcher such as Bretau and Roux did, in fact, obtain bright coatings, which formed, once the reducing agent had been added, on all surface in the reaction vessel. Several years later, Frederic, in a dissertation, described the reaction of nickel salts in alkaline medium with hypophosphite in the presence of palladium activator [8]. All of these studies didn’t lead to any practical application of electroless-nickel. The discovery of electroless-nickel plating technology as it is in use today can be said to have been made in 1944 and patented in 1953 [9] when, after some two years of work, Brenner and Riddell

developed practical system. At that time General American Transportation Corporation further developed the process and marketed it under name “Kanigen” [9]. From year 1978 to 1982 was marked as a further advance in technology, insofar as phosphorus-rich electroless-nickel coatings were developed which were formed as a glassy and amorphous structure [8].

Now a days electroless-nickel is available from many companies for commercial and experimental use. But electroless-nickel with high phosphorus content (%P>13%) is very difficult to achieve and costly also, the other problem is to get high thickness of coating which results in defective surface.

The objective of this chapter is to review the machining history of electroless-nickel and compare the different study and analyze the results.

2.2 STRUCTURE OF ELECTROLESS-NICKEL

Structure of material plays important roles in machining for study of tool wear and surface roughness. The structure of electroless-nickel is mainly dependent on phosphorus content and heat treatment procedure. A. Mayer et al. [10] declared electroless-nickel as a single phase amorphous alloy from x-ray diffraction scan and TEM examination of nickel phosphorus alloy viewed normal to the deposited layer but this amorphous structure changes in low temperature and short incubation time to a two phase material with intermetalics in the crystalline nickel matrix for high phosphorus electroless-nickel. A good idea about structural change in electroless-nickel can be got from the Figure 2.1.

Electroless-nickel plating deposits in a laminar fashion and this lamination can be eliminated and the inherent strength of the plating increased by heat treatment [9].

Rolf Weil et al [11] described that properties determined with a tensile-testing device described by Kim and Weil shows that electroless-nickel is a relatively hard but brittle material, the low ductility is due to the microcrystalline and amorphous structures that are essential preclude plastic deformation and the deformation is therefore mostly elastic until fracture occurs.

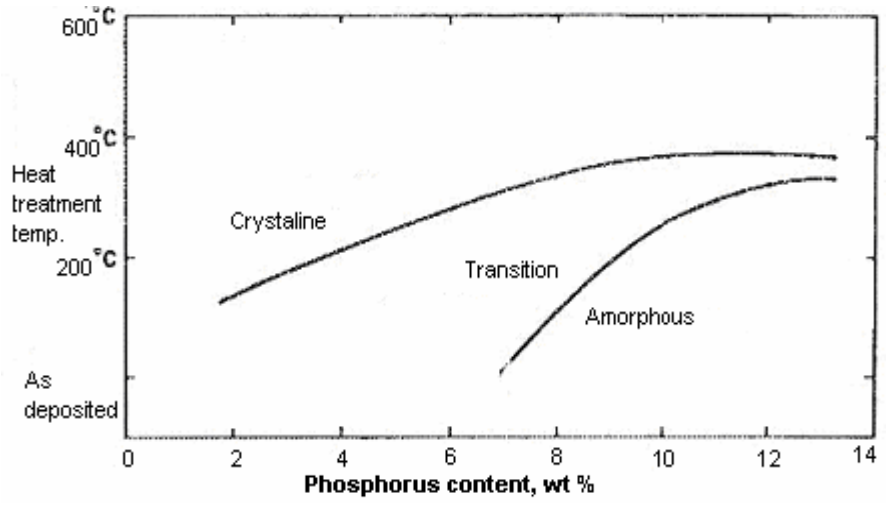

Figure 2.1 Effects of phosphorus content and heat treatment on electroless-nickel structure.

2.3 HARDNESS OF ELECTROLESS-NICKEL

There are so many works regarding the hardness of electroless nickel and from these one could certainly say that hardness is the most widely studied property of electroless-nickel deposits [12]. Hardness, which plays a significant role in selecting the cutting tool material and value of cutting parameters, is mainly controlled by phosphorus content and heat treatment, this fact makes electroless-nickel more attractive in machining world.

The other factors such as residual stress and bonding strength with substrate depend on substrate materials, plating procedure and heat treatment.

According to J.M. Casstevens et al. [9] electroless-nickel may have phosphorus content ranging from 2 to 22 percent. The hardness and residual stress level of the plate are influenced with phosphorus content and continued heat treatment will, depending on temperature, affect the hardness as the Figure 2.2 below.

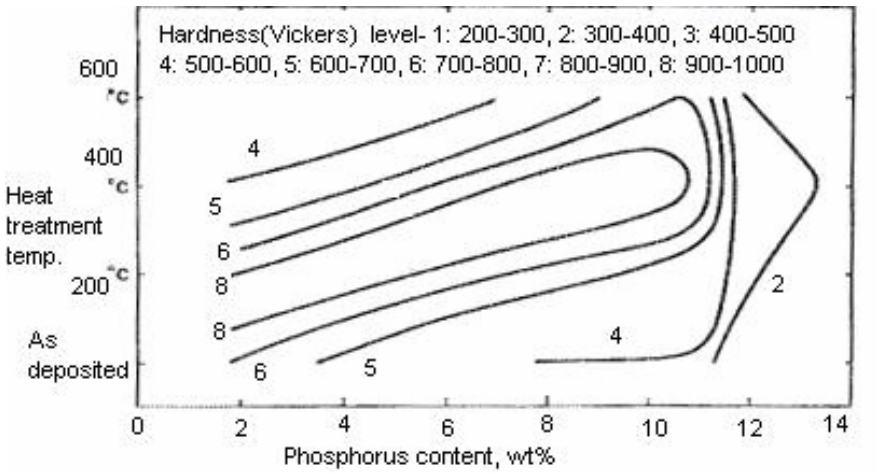

Figure 2.2 Influence of phosphorus content and heat treatment condition on hardness.

G. M. Sanger et al. [4] stated that by judicious choice of operating conditions it is possible to deposit coating that are in stress-free state. Figure 2.3, shows the stress in electroless-nickel deposits as a function of phosphorus content on aluminum and brass, which have high expansion coefficient and steel, beryllium and titanium, which have low expansion coefficients. Besides showing that the substrate has a very distinct influence on stress, the curves also show that for each metal, a deposit with zero stress can be obtained by controlling the amount of phosphorus in the coating.

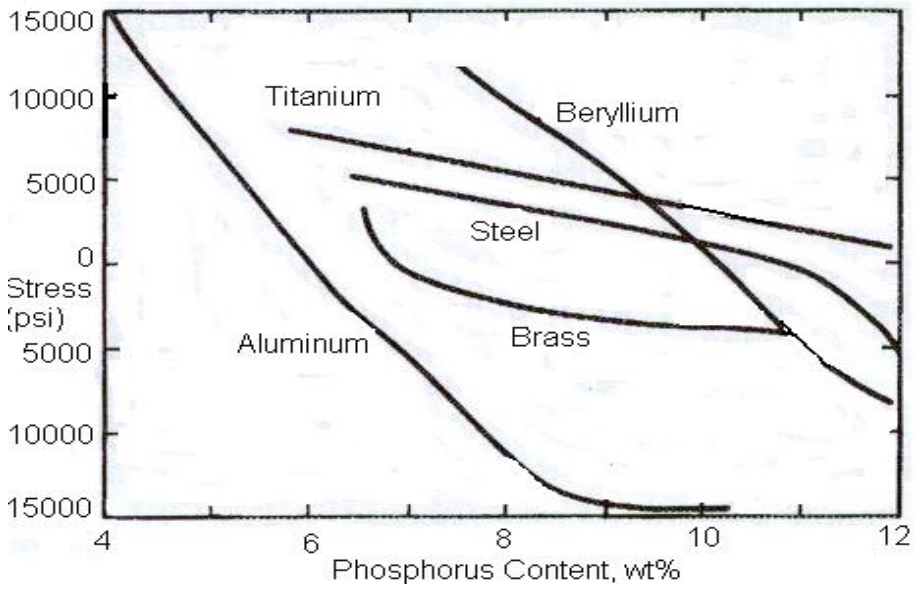

Figure 2.3 Stress in electroless-nickel as a function of phosphorus content on metal with high (aluminum, and brass) and low(steel, beryllium and titanium) expansion coefficient.

2.4 MACHINING OF ELECTROLESS-NICKEL PLATING

Diamond turning of electroless-nickel was first reported in 1978 by J.M. Casstevens et al [9] where an explanation of the electroless nickel-plating process, optical applications, important metallurgical and mechanical properties of plating were given. Machinability tests were conducted with various types of plating, thickness of plating, types of substrates and heat treatment of the plating and results of the testing program were presented. Machining was performed on electroless-nickel plated disk of 102mm diameter at Oak Ridge Y-12 Plant with spindle speed 350 to 1000rpm and feed rate 14.5 to 2.54μm/rev and different round-nose tool (radius of 0.53, 1.60, 3.18 and 25.4mm). The calculated surface finish for typically diamond turning parameters had not been reached. The conclusion was that the tool radius does not greatly affect the measured surface finish of electroless-nickel if the tool advance is matched to the tool radius to give the same theoretical finish. Heat treatment of diamond-turned electroless

nickel in a vacuum furnace appeared to roughen the surface slightly, giving it an oranged-peel appearance when viewed under a surface-finish measuring microscope. Substrate movement might introduce surface-figure distortion. Very little tool wear was noticed and tool life for machining electroless-nickel is about the same as when machining such softer fcc metals as copper and aluminum. Tool life when machining hardened electroless-nickel, might shorten somewhat, although very good finish was machined on heat-treated electroless-nickel.

G. M. Sanger et al [4] in 1982 had discussed the importance of good quality electroless-nickel coating e.g. the absence of surface pits, porosity, nodules, stress and inclusions large enough to damage the diamond tool or adversely affect the machining process emphasized and presented information on influence of plating defects on optics. Electroless-nickel was machined in both the as deposited condition and after heat treatment with iso-statically pressing at 590^0C, 30,000psi, for 2 hours in an argon atmosphere. Turning was accomplished on a Pneumo precision lathe (MSG-326) with 5.08mm nose radius single crystal diamond tool at different depth of cut (1.27µm, 0.5µm, 0.25µm, and two spark out passes). Diamond turning and polishing of other electrodeposited coatings including bright nickel; sulfamate nickel and tin-nickel were performed. Machinability was determined by judging the micro-surface character of machined surface and amount of wear on cutting edge. The result indicated that as deposited electroless-nickel and hot iso-statically pressed plating of electroless-nickel deposit showed promise of diamond machining as an optically specular surface was achieved on them and the tool wear on diamond was negligibly small when viewed under high magnification. It was assumed that the low wear might be for less temperature generation for alloying element as perhaps with the alloy coatings the

diamond tool just doesn't get as it does with unalloyed nickel and heat treatment does not degrade the electroless-nickel for diamond turning.

J. W. Dini et al [5] studied the machinability of electroless-nickel in 1985 with different phosphorus content (1.8% -13%) in as deposited condition and after heat treatment at different temperature (200, 400, and 600^0C). After machining electroless-nickel for very short distance some good conclusions came out. From the result of the experiments it was shown that the machinability of electroless-nickel increases with the increase of phosphorus content in terms of surface finish and tool wear. The increased hardness with heat treatment of high phosphorus content gives best surface. The relationship of heat treatment temperature, phosphorus content and surface finish has been established by the Figure 2.4.

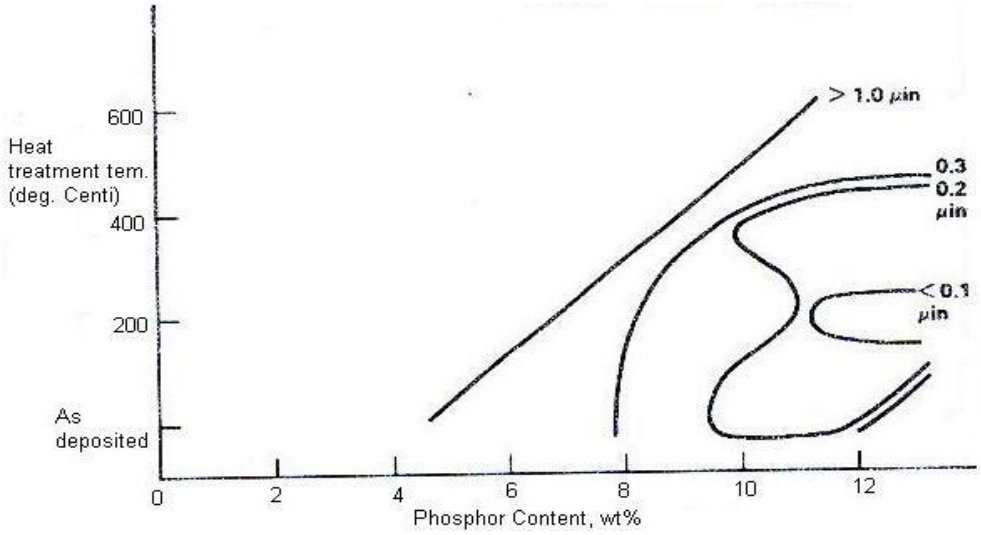

Figure 2.4 Influence of phosphorus content and heat treatment condition on surface roughness.

The machining history of electroless-nickel is very old but the number of work is very few. Though every work was performed in different views and aspects, some similar conclusions arose. From the above discussion it is clear that electroless-nickel becomes harder with heat treatment and gives better surface finish. Electroless-nickel

is very much suited for diamond turning like some other soft material like copper, aluminum etc with very small tool wear.

Form the above analysis it seems that no complete work has been performed on ultra-precision machining of electroless-nickel regarding the effects of machining parameter on machining performance as the machining parameters play very important role in machining economy and surface finish. No effort has been noticed regarding the development of any theoretical model for machining of electroless-nickel.

2.5 TOOL WEAR

There are some reports on diamond tool wear in terms of phosphorus content and heat treatment of electroless nickel for very short cutting distance but none of the reports was in details.

J.M. Casstevens et al [9] reported that the tool life when machining electroless-nickel is about the same as when machining such softer fcc metals as copper and aluminum i.e. wear in diamond cutting tool for turning electroless-nickel is not significant but five times turning of 305mm diameter hemispherical electroless-nickel plate gave only very slight wear when examined under a microscope as with machining the soft metals and tool damage most often results from accidental crushing of ultra-sharp edge rather than from wear. The characteristic of rake wear of diamond tool was presented as in the Figure 2.5.

C. K. Syn et. al. [13] performed some study of diamond tool wear for machining of heat treated (at 200^0C for two hours) electroless-nickel with phosphorus content (13%w/w) where cutting distance was only 21.336km. This work was mainly a comparison of two single crystal natural diamond cutters with different infrared

absorption characteristics, as the absorption characteristics depend on diamond impurity and hardness. The comparison was in terms of surface roughness and tool wear. It was observed that the surface roughness increased rapidly during cutting first 0.3km after that it increased gradually up to 21.34km. Wear of the diamond tool flattened the round-nosed tool tip and sometimes burnishing was occurred rather than cutting. According to this study both micro-fracture and chemical reaction and/or dissolution contribute to the wear of diamond tool edge causing groves at flank face. Of the two tools, the one predicted by infrared absorption measurements to have a higher hardness and lower fracture toughness was found to wear at a lower rate for the first 15.24km and to exhibit somewhat more evidence of edge microfracture. The lower phosphorus content causes scratches at rake face.

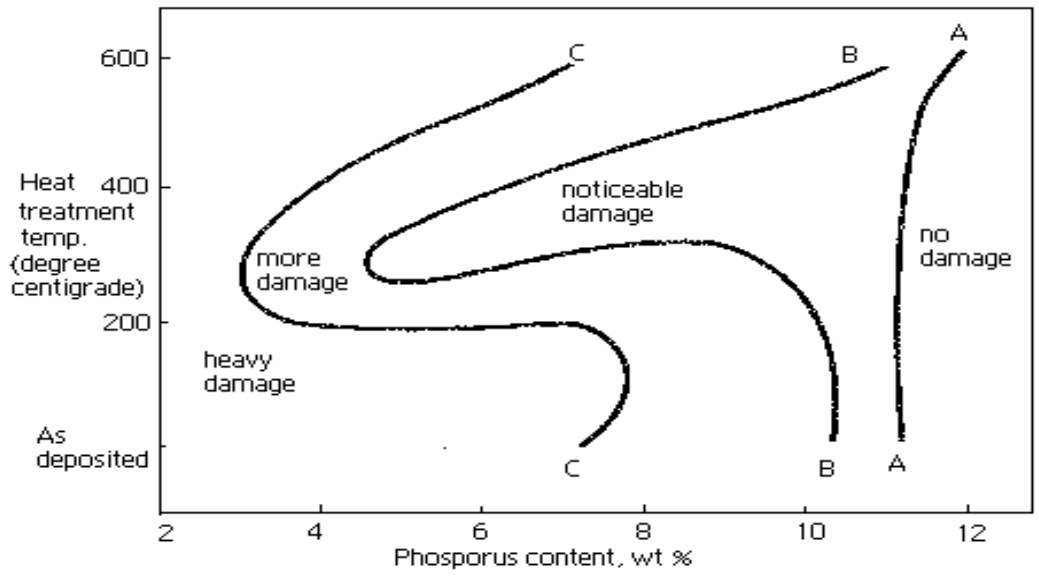

Figure 2.5 Effects of phosphorus content and heat treatment on cutting tool performance.

J. M. Oomen et. al. [14] studied wear behavior of different diamond tools for cutting different materials including electroless-nickel of phosphorus content 9 percent (w/w) where total cutting distance was 50km. Electroless-nickel showed a wear pattern

consisting of several groves or crater wears on the rake face and slight chipping of the cutting edge. The wear was too low to quantify and was nearly same for all type of diamond cutter (synthetic and natural).

There are some works regarding the tool wear but no clear or complete conclusion was drawn. Every time some crater and flank wear were noticed for very short cutting distance and the wear of cutter was mostly attributed to abrasion or microfracture but some researchers also implied chemical wear. Some descriptions regarding tool wear are available but amount and nature of wear with machining was not presented for cutting long distance.

2.6 CONCLUSION

The machining history of electroless-nickel has been divided into five parts and main focus has been given on the machining and tool wear. The conclusions from the review can be stated as follow.

1. The hardness and atomic structure of electroless nickel is dependent on phosphorus content and heat treatment.
2. Heat treatment increases the hardness of electroless-nickel and it depends on temperature and time of heat treatment. Heat-treated electroless-nickel gives better surface finish with worse cutting tool performance.
3. Electroless-nickel is much harder than any other diamond turnable materials like aluminum, copper etc even though it was predicted that the machinability of electroless-nickel is very excellent as other soft materials.
4. Diamond cutter with higher infrared absorption quality experiences lower tool wear.

5. No significant research on tool wear was observed in machining of electroless-nickel. However some results were shown for very short cutting distance where tool wear was very little to measure.

3

THEORETICAL ASPECTS

3.1 INTRODUCTION

It is still a challenge to machine brittle and hard material in ductile mode. To get high quality surface with nano-level finish for glass, ceramic and such other hard materials used in optoelectronics, molding dies etc., it is essential to carry out machining in ductile mode. Otherwise the surface micro-cracks induced by the machining process act as nuclei of fracture. Moreover, a surface machined in ductile mode shows higher strength than that of machined in brittle mode. This chapter deals with the theoretical factors, which affect the mode of machining and explains the ultra-precision cutting behavior of brittle materials.

The chip formation is a process of deformation; forces are subjected by cutting tool upon the work material. The process of deformation involved in chip formation mechanism is in the plastic range. It is known that no permanent effect is produced by stresses within the elastic range. In contrast, stress in the plastic range may cause large deformation. In this range, deformation is no longer a simple separation of atoms, irrecoverable structural changes occur [15]. Broadly speaking, fractures may be classified according to the amount of energy required: brittle fracture requires little energy, and ductile fracture requires much energy. In brittle fracture, the broken parts usually may be refitted together to the original dimensions, with essentially no permanent deformation, the behavior being elastic. In ductile fracture, before rupture there is a considerable plastic deformation that is not recovered, and often it is impossible to refit the severed parts [16].

It is important to note that brittleness and ductility are not absolute properties of materials. The brittleness and ductility change with change in cutting conditions and many other parameters.

The process of brittle fracture consists of three stages [17].

1. Plastic deformation which involves the pile-up of dislocations along their slip planes at an obstacle.
2. The build up of shear stress at the head of pile-up to nucleate a micro-crack.
3. In some cases the stored elastic strain energy drives the micro crack to complete fracture without further dislocation movement in the pile-up. More typically in metals, a distinct growth stage is observed in which an increased stress is required to propagate the micro-crack.

The process of ductile fracture also consists of three stages [18].

1. A stage of nucleation by internal cracking of second-phase particles or inclusions when no void are already available as in the case with sintered materials or with materials with internally cracked particles as is easily the case with coarse particles, or by decohesion at particle-interface.
2. A stage of growth of these voids up to a critical size.
3. A stage of coalescence of these voids that give the final rupture path.

3.2 BRITTLE-TO-DUCTILE TRANSITION

The transition in brittle-to-ductile fracture behavior is an important phenomenon for machining area. Here a theory of the brittle-to-ductile transition has been considered based on the dislocation concepts [17]. Cottrel's equation can be presented as follows showing the important variables in brittle fracture.

$$(\tau_i D^{1/2} + k') k' = G \gamma_s \beta \quad (3.1)$$

Where τ_i = the resistance of the lattice to dislocation movement

k'= a parameter related to release of dislocations from a pile-up

γ_s= the effective surface energy and includes the energy of plastic deformation

β = a term which expresses the ratio of shear stress to normal stress. For torsion 1; for tension ½; for notch $^1/_3$.

D = Diameter of grain.

G = Modulus of rigidity.

Equation (3.1) expresses the limiting condition for the formation of a propagating crack from a pile-up of gliding dislocations. If the left side of the equation is smaller than the right side, a micro-crack can form but it cannot grow. This is the case of non-propagating micro-cracks. When the left side of the equation is greater than the right, a propagating brittle fracture can be produced at a shear stress equal to yield stress. Thus, this equation describes a brittle to ductile transition. The equation is very much complicated as the components of this equation are linked to each other. For the above equation the following factors can be considered effective for transition to ductile mode from brittle mode cutting.

3.2.1 The Brittle-to-Ductile Transition In Grain Size

The yield stress is ruled by the Hall-Petch law and cleavage stress is the stress required for propagation through a grain. This relation has been presented by the following equation [17].

$$\sigma_0 = \sigma i + kD^{-1/2} \quad (3.2)$$

Where σ_0 = the yield stress

σi = the "friction stress" representing the overall resistance of the crystal lattice to dislocation movement.

k = the "locking parameter" which measures the relative hardening contribution of the grain boundary.

D = grain diameter.

For coarse grain-size, when the yield stress is reached the cleavage stress is overtaken and brittle fracture occurs without any ductility. Moreover the accurate determination of yield stress is only possible in compression, because in tension the surface defect triggers off the fracture prematurely. For fine grain-size, the critical stress is only reached with the help of strain hardening and the ductility expressed here in terms of reduction of area or necking, increases with a decreasing grain size. For grain-size still smaller, fracture is purely ductile and failure of the specimen is occurs by necking.

3.2.2. The Brittle-to-Ductile Transition In Temperature

For every material there may be three transition temperatures. At low temperature brittle fracture occurs as soon as the yield stress is reached either by twining or by gliding. At intermediate temperatures, the cleavage stress is only reached with strain hardening and ductility appears. At higher temperature, cleavage is ruled by the grain boundary crossing and several micro-cracks develop [18]. The temperature mainly affects on modulus of rigidity, effective surface energy and resistance of lattice to dislocation movement. With the increase of temperature hardness of materials decreases which leads to ductile mode machining.

3.2.3 Hardness of materials

Hardness of any material is very much dependent on the temperature of that materials. The temperature generation for a cutting process can be formulated in the following equation [19].

$$\theta e = [(1-\Gamma)\, Fc + (\Gamma-1+A)\, F_f\, r_c] / \rho c a_c a_w + \theta_0 \qquad (3.3)$$

Where θe = temperature in chip formation zone.

θ_0 = initial workpiece temperature.

Γ = proportion of heat conducted from chip formation zone to workpiece.

A = cutting edge temperature rise factor amplitude.

F_c = cutting force in cutting direction.

F_f = friction force on tool face.

r_c = ratio of undeformed chip thickness to chipthickness

a_c = undeformed chip thickness.

a_w = width of cut.

ρ = workpiece density

c = workpiece specific heat capacity.

The hardness of work material H is a function of temperature in the cutting region, i.e.

$$H = f(\theta e) \qquad (3.4)$$

Generally all hard materials are brittle and soft materials are ductile. With the increase of temperature the atomic kinematics of materials changes by softening the materials with increasing ductility.

3.2.4 Brittleness of materials

The brittleness of material is inversely to ductility but no distinct line to separate materials as ductile or brittle. Generally brittleness may be indicated in terms of fracture toughness, which is a material property of the ability to resist the growth of a pre-existing crack or flaw from where the brittle fracture starts. The following equation is used to calculate the fracture toughness of materials [20, 21].

$$\left(\frac{K_{IC}\Phi}{Ha^{0.5}}\right)\left(\frac{H}{E\Phi}\right)^{0.4}\alpha = \left(\frac{c}{a}\right)^{\left(c/18a\right)-1.51} \tag{3.5}$$

Where $$\alpha = 14\left\{1-8\left(\frac{4\nu-0.5}{1+\nu}\right)^{4}\right\} \tag{3.6}$$

α = non dimensional constant related to poisson's ratio

Φ = constraint factor ≈ 3

H = hardness

E = young Modulus

ν = poisson's ratio

K_{IC} = fracture toughness

c = crack length

a= half of the average. of two diagonals of the indentation mark

3.2.5 Defects in materials

Brittle fracture is mainly initiated by some imperfection such as microscopic crack or void which causes a stress concentration near the crack. If this high value of stress equals the cohesive strength of materials, the atomic bonds at that region would be overcome. As they are broken, the previously localized imperfections spread across the material causing fracture [16].

The energy balance for brittle fracture can be developed mathematically [16]. Consider events during an increment of cracking where the external displacement of the cracked structure is $\Delta\delta$ and the associated increment of crack area is ΔA (Figure 3.1). Work done by external load $P\Delta\delta$, and the crack absorbs energy $R\Delta A$. The strain energy Λ of the structure changes by $\Delta\Lambda$. This energy change can be given by $\Delta\Lambda=\Delta^{1}/_{2}(P\delta)$.

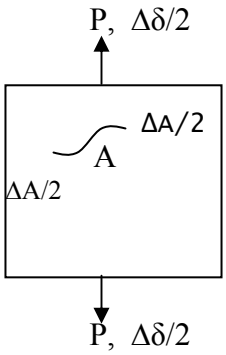

Figure 3.1 The effect of crack with application of load

Thus, equating the rate of doing external work to that of doing internal work for quasi-static cracking and neglecting kinetic effects, we have

$$P\,\Delta\delta = \Delta\Lambda + R\,\Delta A = \Delta\left({}^{P\delta}/_{2}\right) + R\,\Delta A$$

Hence, $$P\,\Delta\delta = {}^{1}/_{2}P\,\Delta\delta + {}^{1}/_{2}\delta\,\Delta P + R\,\Delta A$$

So, $P\,\Delta\delta - \delta\,\Delta P = 2R\,\Delta A$

Dividing both side by P^2, We obtain

$$^{d}/_{dA}(^{\delta}/_{P}) = {}^{2R}/_{P}{}^{2}$$

That is,

$$P^2_{crack} = {}^{2R}/_{\{d/dA(\delta/P\}} \qquad (3.7)$$

Equation (3.7) describes the relationship among P, δ and A during cracking. The quantity {d/dA(δ/P)} is the rate of change in compliance of the cracked structure with respect to increase in crack area. Here R can be replaced by K, the critical strain energy released rate. K is also known as stress-intensity factor can be presented as,

$$K = \sigma\,\sqrt{(\pi L)}\sqrt{[\{2b\tan^{-1}(\pi L/2b)\}/\,\pi L]} \qquad (3.8)$$

for the Figure 3.2 below.

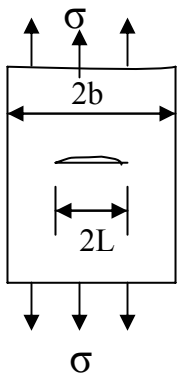

Figure 3.2: A center-crack panel of finite width 2b with crack length 2L laded in axial direction perpendicular to the crack.

3.2.6 Undeformed chip thickness

According to Griffith fracture propagation criterion, the formula for the prediction of a critical depth-of-indentation is of the form [19]

$$d_c = ER / H^2 \tag{3.9}$$

Where d_c is the critical undeformed chip thickness or the critical indentation depth, H is the material hardness and R is the material's fracture energy. One approach to define the fracture energy at small scales is to replace it with a dimensionally analogous measurement of the energy needed to propagate cracks, namely,

$$R \sim K_c^2 / H \tag{3.10}$$

In indentation, the quantity K_c^2 / H is considered as an effective measurement of the brittleness and K_c is the fracture toughness. This quantity can be substitute in to equation (3.8) to yield

$d_c \propto (E / H)(K_c / H)^2$ or

$$d_c = u(E / H)(K_c / H)^2 \tag{3.11}$$

Where u is the brittle-ductile transition factor of the material, depending upon material properties.

Equation (3.11) indicates that in cutting of materials there is a critical value of undeformed chip thickness or depth of cut, below which the chip formation will be in ductile mode. Otherwise, the chip formation is in brittle mode. The critical vale is a function of workpiece material hardness and fracture toughness, which both vary with the temperature in the cutting region.

3.2.7. Tool geometry

Tool geometry has great effect on the cutting mode for same material. The diamond tool sharpness is a primary factor affecting the cutting deformation and the machined surface quality in cutting. The parameter among tool geometry, which mainly affects the brittle-to-ductile transition, is cutting edge radius. The cutting edge radius limits the minimum undeformed chip thickness and the relation between cutting edge radius and minimum undeformed chip thickness can be formulated by the following equations [22].

$$a_{cmin} = \rho\left(1 - \frac{F_t + \mu F_c}{\sqrt{(F_c^{\,2} + F_t^{\,2})(1+\mu^2)}}\right) \qquad (3.12)$$

Where a_{cmin} = minimum undeformed chip thickness

ρ = cutting edge radius of cutting tool

F_t = thrust force.

F_c = cutting force.

μ = coefficient of friction.

It is generally known that for every material there is a critical depth of cut for which brittle-to-ductile mode machining happens and the lesser the depth of cut the more ductile the machining mode. Shoichi Shimada et. al.[23] have concluded that the movement of cavities shows the presence of elastic and/or thermal shock waves propagated repeatedly from the cutting tool tip to specimen interface. Because the energy of this shock wave will be supplied by the potential energy stored in the specimen around the cutter tip, it may have enough value to create micro-crack when the scale of indentation of machining is increased. In that case, some pre-existing

defects and/or free surface may play a crucial role for the enhancement of the intensity of the shock wave by reflection and/or interference. In the other words, when a depth of cut in a unit process of machining is kept very small, that the shock wave can not supply the necessary energy to initiate crack nuclei or to propagate the pre-existing crack, there is a little possibility of a brittle mode machining.

The critical depth of cut depends mainly on material property, depth of cut and cutting edge radius and for brittle- to-ductile transition each material has constant value of the ratio, cutting edge radius to undeformed chip thickness [19].

3.2.8 Effect of coolant and mist

Coolant and mist are well known as for lubrication and reducing temperature at the machining zone. These factors also prevent chips deposition at the cutting area and keep the machined surface clean.

3.3 CONCLUSION

Various factors that have control on ductile to brittle transition have been described in this chapter. Electroless nickel is a well-known brittle material, so the theoretical knowledge to machine electroless nickel in ductile mode is important. If the workpiece material and tool geometry are fixed then the brittle-to-ductile transition phenomenon comes under control of machining parameters. During experiments cutting conditions and workpiece material's composition are taken into consideration.

4

EXPERIMENTAL SETUP AND PROCEDURE

4.1 EXPERIMENTAL SETUP

A photographic view of experimental setup is shown in the Figure 4.1, which gives a clear idea about the positioning of mist spray nozzle, workpiece, cutting tool, chip suction nozzle and force dynamometer.

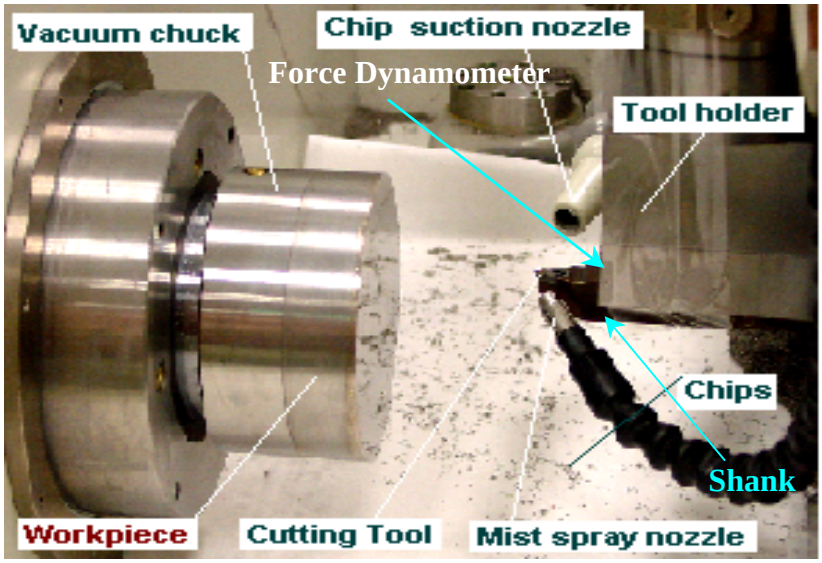

Figure 4.1: Photographic view of experimental set-up

Experimental setup is mainly composed of the following parts.

1. Toshiba Ultra-precision machine
2. Single point diamond cutting tool
3. Workpiece
4. Cutting force data acquisition system.
5. Chip collection system

4.1.1 Toshiba Ultra-precision machine

The Figure 4.2 shows the picture of TOSHIBA ultra-precision machine; model ULG-100H[3], which was used to perform all the experiments. The Kerosene based mist spray system, chip suction system and force measurement system were attached with this machine around the machining unit as described in the Figure 4.1.

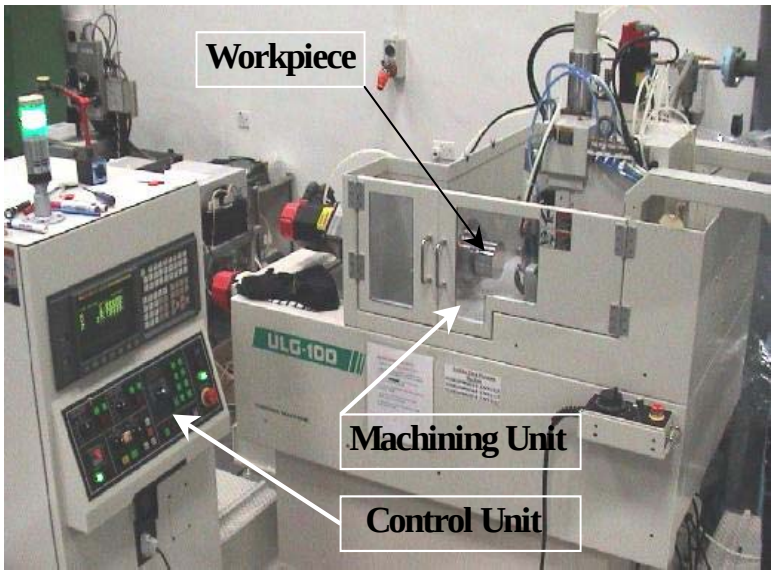

Figure 4.2: Ultra-precision machine

4.1.2 Single point diamond cutting tool

Round nosed diamond cutting tools of two types i.e. artificial and natural diamond were used in the ultra-precision machining. Figure 4.3 shows a picture of artificial diamond cutter. All the cutters were of 0 degree rake angle, 7 degree flank angle and 2mm nose radius.

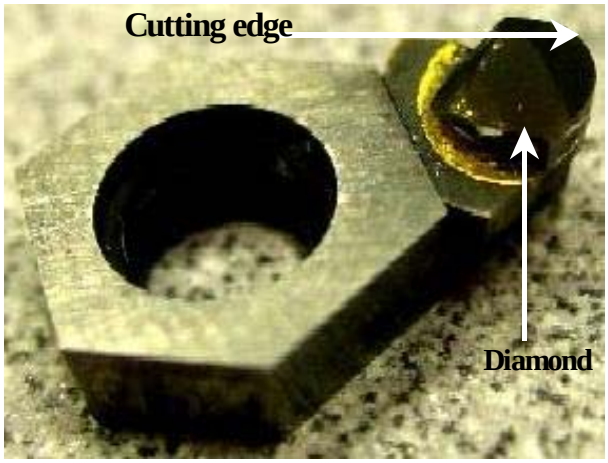

Figure 4.3: Artificial diamond cutting tool (insert)

4.1.3 Workpiece

Electroless-nickel was used as workpice material in this project. Electroless-nickel of 100µm thickness was plated on starvax workpiece of 100mm diameter and 20mm thickness with a con-centric recess of 5mm diameter at the center. Figure 4.4 shows the picture of workpieces. All the workpieces were bought from market then the surface was prepared for final experiments after ensuring a very good flat surface by trimming off several thin layers of electroless-nickel from top.

Figure 4.4: Workpiece

4.1.4 Cutting force data acquisition system

Cutting force and thrust force were measured during machining with a Kistler piezoelectric 3-componenet slim dynamometer in conjunction with a Kistler 3-channel digital charge amplifier and a recorder to record the forces. Cutting forces are recorded using a Sony PC 208Ax data recorder and are processed by using PC Scan MK II data acquisition software. The sampling frequency of digital cutting force data acquisition is 24kHz and is recorded using a Sony data cartridge of 1.3GB capacity inserted in the Sony data recorder.

4.1.5 Chip collection system

The chips were collected to facilitate clean cutting and prevent any chip deposition on cutting tool or workpiece surface. This system consists of a compressor, suction pipe and nozzle.

4.2 EXPERIMENTAL PROCEDURE

The picture of experimental set-up is shown in the Figure. 4.1. Workpiece was attached to the spindle by vacuum and was balanced with the help of a dial indicator. The inserts were mounted beneath the slim dynamometer, which was screwed with tool holder. The machining can be divided in to four major parts and these are -

1. Finding the effect of cutting conditions and workpiece materials
2. Checking wear characteristics of natural and artificial diamond cutting tools.
3. Effect of different phosphorus contents in work pieces on diamond cutter.

4. Effect of depth-of-cut on cutting tool performance.

For all the experiments, measurements and observations made included:

a) Plunge cuts on oxygen free high conductivity copper were performed before and after every experiments to observe any change in tool profile during cutting
b) Measurement of hardness (Hv) to see the effects of hardness on machining,
c) Optical observation of the cutting tools and electroless-nickel surface with Nomarski microscope.
d) Every machined surface was measured with a telystep stylus profiler with an added computer data acquisition system for calculation of the arithmetic mean surface roughness (R_a) and the maximum pick-to-valley height within the assessment length (R_y).

4.2.1 Finding the effect of cutting conditions and workpiece materials

The machining procedure was chosen primarily to determine the influence of depth of cut, the feed rate and spindle speed on three workpieces of different phosphorus contents on the surface finish and cutting forces. The parameter matrix for the experimental studies would include four depth of cuts (2µm, 4µm, 7µm, 10µm), four feed rates (2µm/rev, 10µm/rev, 30µm/rev, 50µm/rev), four spindle speeds (100rpm, 500rpm, 1000rpm, 1500rpm), and three different phosphorus contents (10.23, 9.57 and 8.47 %w/w).

In the first set of experiments, depth of cut was varied and while the spindle speed (1000rpm), feed rate (10µm/rev) and phosphorus content (9.57%w/w) were kept constant. For the second set of experiments, feed rate was varied while the depth of cut (4µm), spindle speed (1000) and phosphorus content (8.47%w/w) were kept constant.

In the same way for the last set of experiments spindle speed was varied while the depth of cut (4µm), feed rate (10µm/rev) and phosphorus content (10.23%w/w) were kept constant. The experimental details are given in the Table 4.1.

Table 4.1 Test conditions to see the effects of cutting parameters.

Exp No.	Depth of cut (µm)	Feed rate (µm/rev)	Spindle speed (rpm)	Phosphorous content (% w/w)
1	2	10	1000	9.57
2	4	10	1000	9.57
3	7	10	1000	9.57
4	10	10	1000	9.57
5	4	2	1000	8.47
6	4	10	1000	8.47
7	4	30	1000	8.47
8	4	50	1000	8.47
9	4	10	100	10.23
10	4	10	500	10.23
11	4	10	1000	10.23
12	4	10	1500	10.23

4.2.2 Wear characteristics of different types of diamond cutting tools

The cutting conditions for natural and artificial diamond cutter were as in the Table 4.2. Cutting tools were traveled from periphery to the center of workpiece and experimental data was taken after 1^{st}, 2^{nd}, 3^{rd}, 10^{th}, 20^{th}, 40^{th} pass and then after every 20 passes up to 260^{th} pass, manual observation was performed after every pass.

Table 4.2 Test conditions to see performance of natural and artificial cutter

Types of Diamond	Depth of cut	Feed rate	Spindle speed	Phosphorus content
Artificial	2µm	10µm/rev	1000 rpm	10.5%w/w
Natural	2µm	10µm/rev	1000 rpm	10.5%w/w

4.2.3 Effect of different phosphorus contents on diamond cutter

The cutting conditions to test the effect of phosphorus on cutter performance are given in the Table 4.3. This time like the last section cutting tools were traveled from periphery to the center of workpiece and experimental data was taken same way as before after 1^{st}, 2^{nd}, 3^{rd}, 10^{th}, 20^{th}, 40^{th} pass and then after every 20 passes up to 260^{th} pass, manual observation was performed after every pass.

Table 4.3 Cutting conditions to investigate the effect of phosphorus content

Types of Diamond	Depth of cut	Feed rate	Spindle speed	Phosphorus content
Artificial	2µm	10µm/rev	1000rpm	5.8%w/w
Artificial	2µm	10µm/rev	1000rpm	11.5%w/w

4.2.4 Effect of depth-of-cut on cutting tool performance

To investigate the effect of depth-of-cut, one artificial diamond cutter was used with 4µm depth of cut for cutting 200km. The cutting conditions were as in the Table 4.4 and the results were compared with that of artificial diamond cutter in the Table 4.2.

Table 4.4 Cutting conditions to investigate the effect of depth-of-cut

Types of Diamond	Depth of cut	Feed rate	Spindle speed	phosphorus content
Artificial	4µm	10µm/rev	1000rpm	9-13 %w/w

During experiments the cutting tool was made to travel from periphery to the center of workpiece and experimental data was taken after 1^{st}, 2^{nd}, 5^{th}, 10^{th}, 20^{th}, 50^{th} pass and then after every 15 passes up to 260^{th} pass. Manual observation was performed after every pass.

4.3 DATA PROCESSING AND CALCULATION TECHNIQUE

4.3.1 Measurement of surface roughness

The workpiece surface was divided into three regions and in every region 5mm data length was selected. The value of the surface roughness (R_a and R_t) from Talysurf was recorded directly for every data length and the average value of the three regions was taken as the surface roughness of that surface.

4.3.2 Measurement of cutting forces

All the force data were recorded from the data cartridge by using a tape recorder, interface and a computer using PC Scan MK II software. Real time plot of forces were monitored and selected at desired zone, normally at the start of cutting. Then the desired data were exported and saved as ASCII-tab files. These data were retrieved in Microsoft Excel for further analysis.

4.3.3 Taking picture of cutter and surface, and Measurement of tool wear

All the pictures of machined surface and cutting tool faces were taken directly from Nomarski microscope using a digital camera then these pictures were transferred and saved as jpeg file in the computer for further analysis.

The wear was observed and measured directly by using Nomarski microscope and its scale is in nano-metric level. The depth of rake wear was very small but the area of

wear was comparatively large and cosequently it was difficult to measure the depth of wear. In this project rake wear has been expressed in terms of area of the wear.

4.4 EQUIPMENT USED

4.4.1 Nomarski Microscope (OLYMPUS STM 6 Measuring Microscope)

Nomarski microscope in the Figure 4.5 was used to observe machined surface, cutting tool wear and to measure tool wear. This microscope can be used only for two types of magnification i.e. 100times and 500times.

Figure 4.5 STM optical and measuring microscope

4.4.2 Talystep Stylas Profilometer (Taylor-Hobson)

Taylor-Hobson Surface profilometer of Form Talysurf-120 in the Figure 4.6 was used to measure roughness of machined surfaces. The stylus Taylor-Hobson profilo-meter was made to travel on the surface from outer to inner side with a speed of 1mm/sec. The parameters used during measurement were as follow.

Filter: Gaussian Data length: 5mm Cutoff (Lc): 0.08

Cutoff (Ls): 0.0025 Band width: 30:1

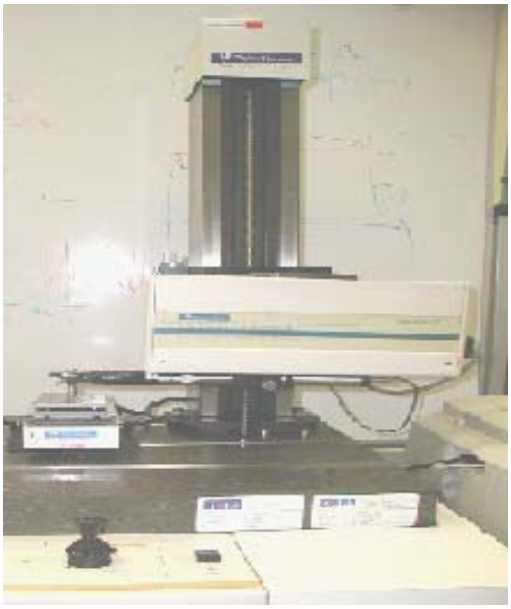

Figure 4.6 Taylor Hobson Surface tester

5

RESULTS AND DISCUSSION

5.1 INTRODUCTION

Being one of the most modern manufacturing processes, there has been substantial interest in investigation on ultra-precision turning and in the world of ultra-precision finishing of electroless-nickel which is used extensively where hard, stable, corrosion resistance and nano-level surface finish are essential. Electroless-nickel is generally used for molding dies of plastic optical parts such as LCD or projection TV, magnetic memory drive, laser equipment, electrostatic copier, printing machine [24]. So it is important to investigate the effects of machining parameters on ultra-precision turning of electroless nickel and the performance of different diamond cutter in machining of electroless nickel with different phosphorus content and machining conditions.

The objectives of this chapter are to present and discuss

(i) The effects of machining conditions and phosphorus content on the surface finish, surface appearance and cutting forces.

(ii) The wear characteristics of different types of diamond cutter for very long cutting distance.

(iii) The effect of phosphorus content on the performance of artificial diamond cutter.

(iv) The effect of depth-of-cut on the performance of artificial diamond cutter.

5.2 EFFECTS OF MACHINING PARAMETERS AND PHOSPHORUS CONTENT ON MACHINING PERFORMANCE

Choosing proper machining condition is very essential for any machining process, so the effect of machining parameters should be known. Here feedrate, phosphorus content, spindle speed and depth-of-cut have been chosen to see their effect on surface roughness, surface appearance and cutting forces.

5.2.1 EFFECT OF FEED RATE

Surface roughness of ultra-precision machining is largely influenced by machine kinematics at high feed rate, but significantly influenced by other factors at lower feed rate [25]. In face turning, the surface roughness profile across the diameter of workpiece can be determined by the tool geometry (nose radius and cutting edge angle) and feedrate. The impact of these factors is depicted by Groover (1996, p.635)[26]. Past computational studies have been reported recently by Groove (1996) and Boothroyd and Knight (1989)[27]. For ideal conditions, the surface roughness profile is formed by the repetition of tool profile at intervals of feed per workpiece revolution. For clarity of presentation, the most notable models for estimating the ideal surface roughness in turning are briefed next. Assuming a non-zero cutter nose radius (r), The following equation is used to estimate the ideal roughness value (Groove 1996, p.634 and Boothroyd and Knight 1989, p.166)

$$R_a = \frac{f^2}{32r} \tag{5.1}$$

Where: R_a = ideal arithmetic average surface roughness (in. or mm), f = feed (in./rev or mm/rev) and r = cutter nose radius [27]. This equation gives a roughness value in in. or mm that can be converted to micro inch or μm. This equation assumes that the feed and

nose radius are the principal factors that determine the geometry of the surface. If the nose radius would be zero, then Equation 5.2 is estimate the ideal surface roughness (Boothroyd and Knight 1989, p.168)

$$R_i = \frac{f}{4(\cot\alpha + \cot\beta)} \tag{5.2}$$

Where α and β are the working major cutting edge angle and end cutting edge angle respectively. To modify the ideal surface roughness value in the form of root mean square (RMS), two additional factors: speed and work piece materials should be considered [28]. In this study round nose cutter is used so Equation 5.1 should be considered for calculation of surface roughness.

One thing should be remembered that the measurement system interferes in the measured surface roughness with changing filtering values. In this study surface roughness increases rapidly with the increase of federate and the plotting of surface roughness (Ra) versus feed rate is shown in the Figure 5.1. The pictures from Nomarsky microscope at Figure 5.2, illustrates the effects of feed rate on surface appearance. It is clear from the picture of surfaces that higher feed rate produces very rough surface.

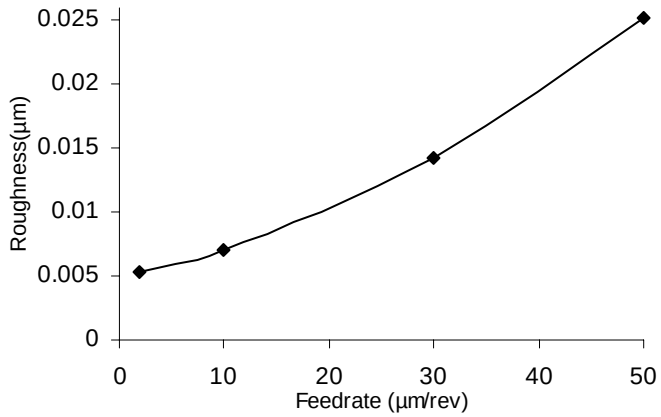

Figure 5.1: Effect of federate on surface roughness

(a) 2µm/rev

(b) 10µm/rev

(c) 30µm/rev

(d) 50µm/rev

Figure5.2: Picture of surfaces at different feed rate from Nomarsky microscope

5.2.2 EFFECTS OF PHOSPHORUS CONTENT

Figure 5.3, shows that surface roughness decreases with the increase of phosphorus content and this may be due to lower hardness and more ductile behavior of electroless-nickel with high phosphorus content [5, 29], one speculation can be introduced is that the phosphorus in the electroless-nickel may act as lubricant and this may also be a factor to get better surface with higher phosphorus content. It seems that a very thin layer of phosphorus covers the cutting edge, which facilitates lubrication and protection of cutting edge form wear [30].

The picture of surfaces for different phosphorus contents do not indicate any thing clearly regarding effect of phosphorus on appearance of surface but from a very careful observation it can be said that higher phosphorus content gives smoother appearance. Here the range of phosphorus content is very small that's why difficulty arose to find out difference among those. Figure 5.4 presents pictures of surface for different phosphorus content.

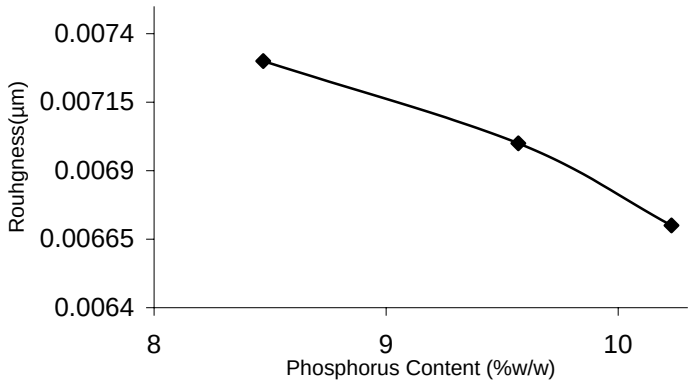

Figure 5.3: Effect of phosphorus content on surface roughness.

(a) 8.47

(b) 9.57

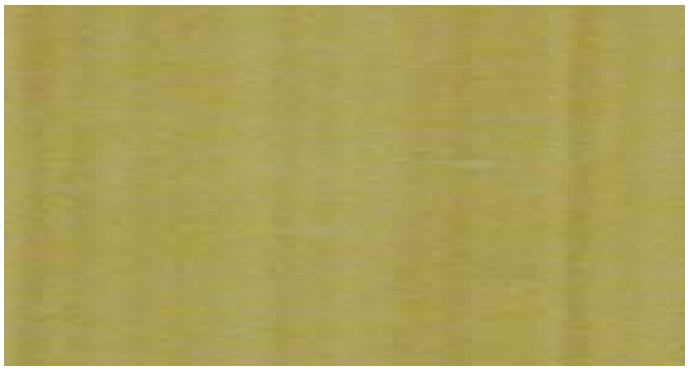

(c) 10.23

Figure 5.4: Picture of surfaces with different phosphorus contents (%w/w), taken by Nomarsky microscope

5.2.3 EFFECT OF SPINDLE SPEED

The effects of spindle speed on surface roughness (Ra) have been shown in Figure 5.5. In the first stage, the surface roughness is in decreasing trend with the increase of spindle speed and after certain limit surface roughness increases very slowly with the increase of spindle speed. With the increase of spindle speed the width of shear zone decreases [15] which leads to less residual stress and fracture in surface but with further increase of spindle speed the vibration of machine tool may increase, this may result in a bad surface. The pictures of surfaces at Figure 5.6 do not indicate any significant effect of spindle speed on surface appearance.

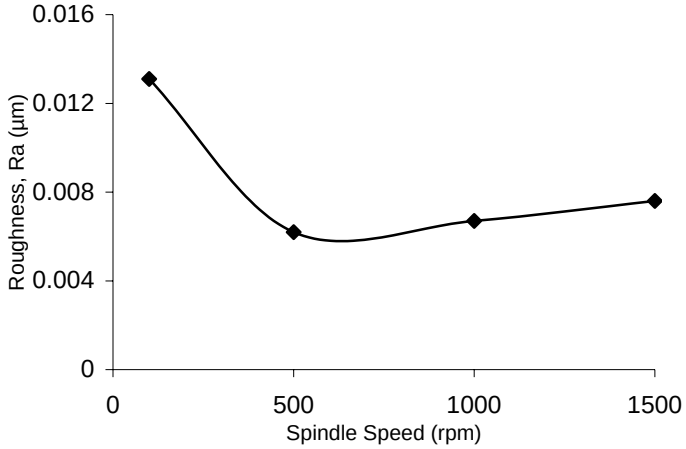

Figure 5.5: Effect of spindle speed on surface roughness.

(a) 100rpm

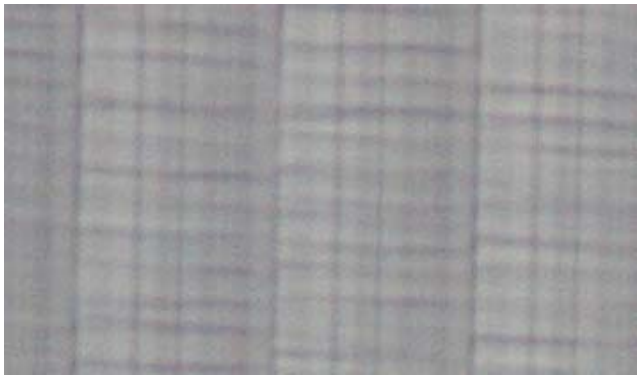

(b) 500rpm

(c) 1000rpm

(d) 1500rpm

Figure 5.6: Picture of surface for different spindle speed.

5.2.4 EFFECT OF DEPTH OF CUT

Surface roughness (R_a) was observed with the variation of depth of cut keeping other factors constant and the plotting of surface roughness versus depth of cut is given in Figure 5.7.

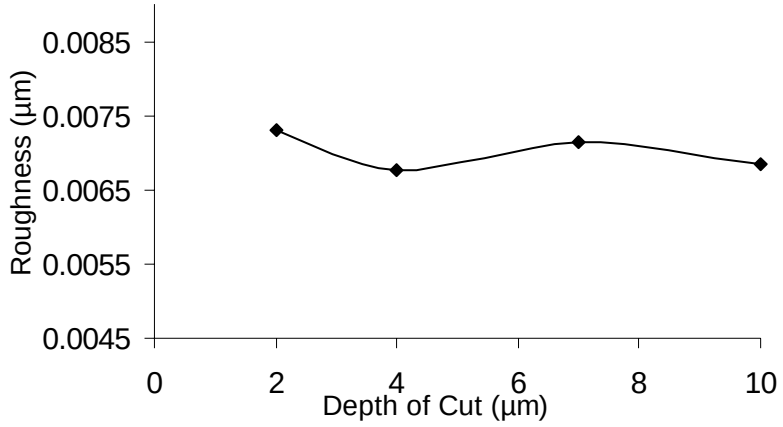

Figure 5.7: Effect of depth of cut on surface roughness.

The graph shows very irregular behavior of surface roughness with depth of cuts and it seems that depth-of-cuts do not play any significant role on surface roughness in this range. In the pictures of surface by Nomarski microscope in the Figure 5.8, do not show any brittle fracture of surface for depth of cut 2µm to 10µm. Electroless-nickel is a brittle material and for brittle material there is a critical depth of cut for transition to brittle mode cutting from ductile mode cutting [31,32], in this instance it seems that the critical depth of cut for electroless-nickel is above 10micron.

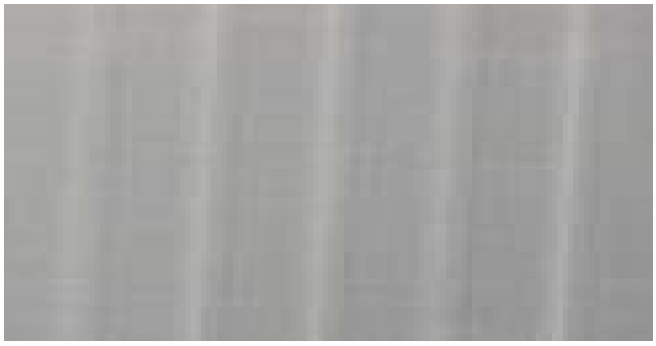

(a) 2μm

(b) 4μm

(c) 7μm

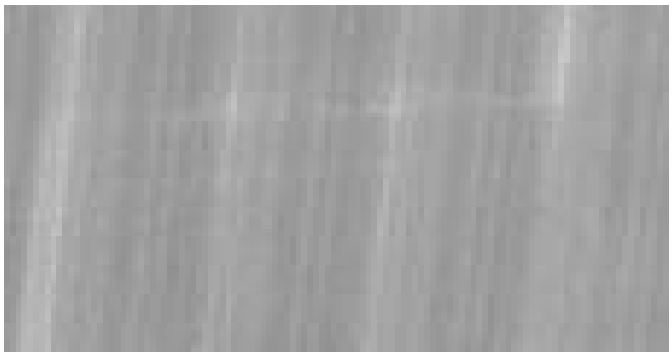

(d) 10μm.

Figure 5.8 Picture of surface for different depth of cut from Nomarski microscope

5.2.5 CUTTING FORCES

The measured two components of forces were (a) Cutting force; normal to cutting tool face and (b) Thrust force; normal to work piece surface. Both of these forces presented here just after the start of cutting and the variation of these forces with variation in the machining parameters can be seen by the following graphs in the Figure 5.9. The graphs indicate that both of these forces increased with the increase of feed rate but forces decreased with the increase of phosphorus content of workpieses. With the increase of feedrate the contact area between tool and workpiece increases, which results in more friction and also the removal of more materials from the workpiecs contributed to the increase in forces. The increase in phosphorus content of the workpiece makes it softer resulting in lower machining forces with higher phosphorus content.

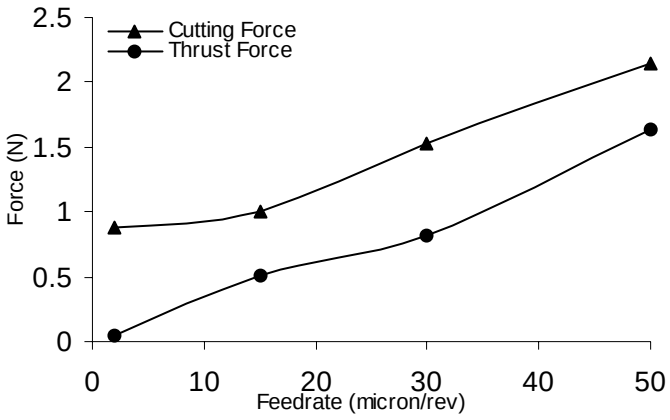

(a) Effect of feedrate on forces

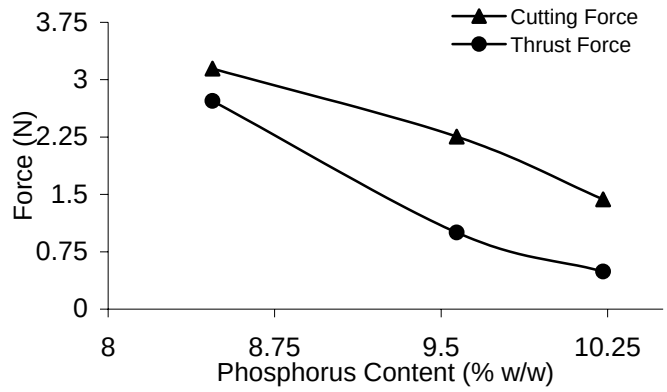

(b) Effect of phosphorus content on forces

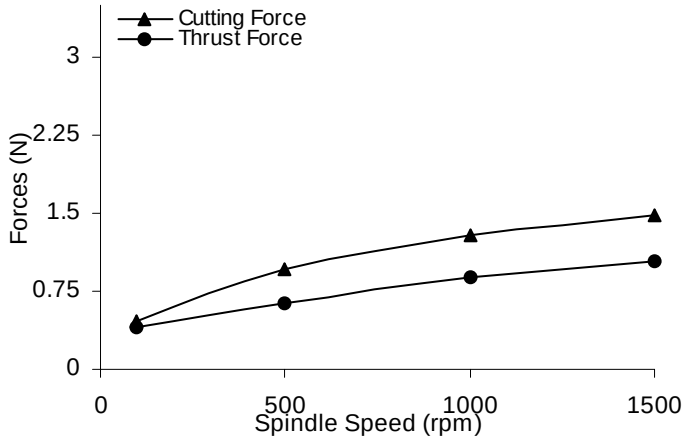

(c) Effect of speed on forces

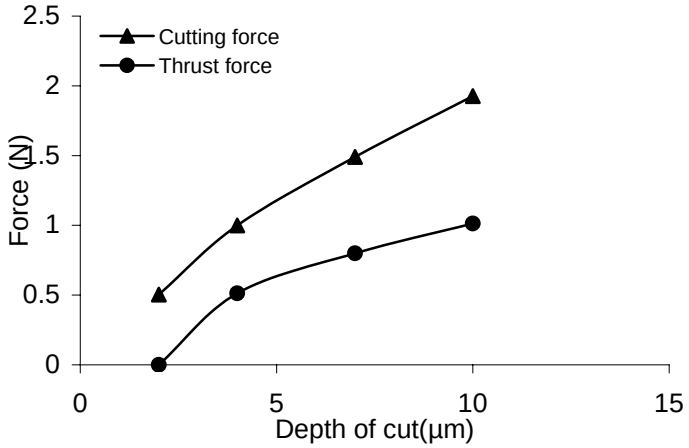

(d) Effect of depth of cut on forces

Figure 5.9: Effect of different cutting parameters on forces

5.2.6 CUTTING TOOL AND WEAR

Cutting edge profile was observed by performing plunge cut test on copper disc and rake faces were observed by Nomarski microscope. No defect on rake face of cutting tool was observed by Nomarski microscope. The cutting distance for every cutting edge was not more than 4 km that is too short for diamond tool to have any wear and no tool defect was observed during experiments for each pass. Plunge test on copper plate did not give any significant information regarding change of cutting edge profile or tool wear. In Figure 5.10, pictures of cutting tool have been shown in the normal to rake face. The bright line presents the cutting edge and no defect in cutting edge is visible after cutting. Here feed direction is upwards and the left side region of cutting edge in every picture is rake face.

Diamond is the hardest material and electroless-nickel is chemically inert, the inertness arises from the absence of geometric defects, as has been suggested to explain the high resistance which some materials exhibit in amorphous state [33], so possibility of any wear is very low. However some wear had appeared at the rake face and flank face and spread to some extent with a sequence of repeated cutting.

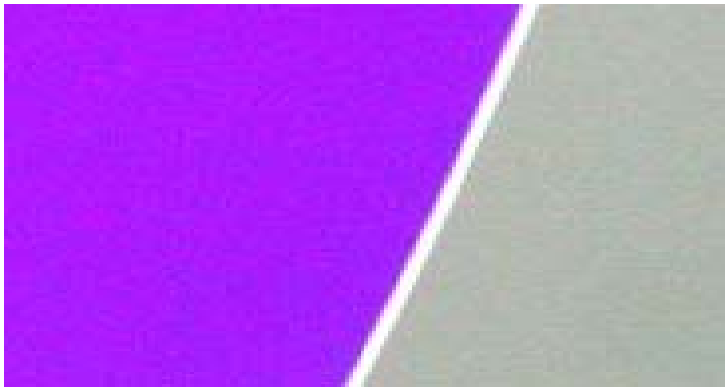

(a) Before cutting

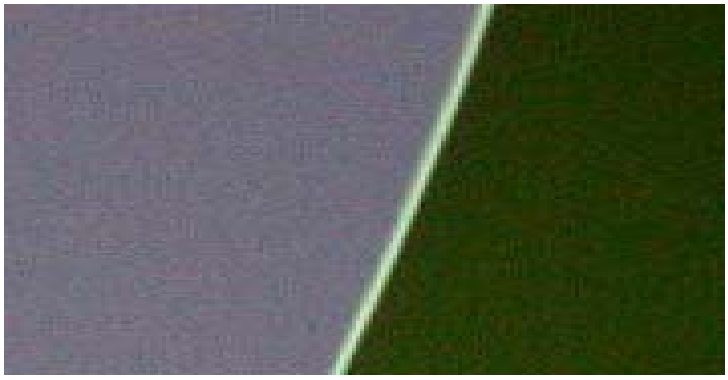

(b) After cutting

Figure 5.10: Picture of cutting edge at rake face from Nomarski microscope.

5.3 WEAR CHARACTERISTICS OF DIFFERENT TYPES OF DIAMOND CUTTER

Two types of diamond cutter i.e. artificial diamond and natural diamond cutter were used to test their performance in terms of rake wear, flank wear, surface finish and cutting forces. The objectives of this section are to present the performance of artificial and natural diamond cutting tools and to compare them in terms of tool wear, surface roughness and cutting forces for 200km cutting distance on electroless nickel plating.

5.3.1 CUTTING TOOL WEAR

5.3.1.1 Natural diamond

Figure 5.11 shows that the flank wear developed as bright line under Nomarski microscope observation with some grooves at 10μm spacing, a value similar to the feedrate. The growth of crater wear at different cutting distance can be described best by the Figure 5.12. The nature of crater wear is quite interesting for its wavy form on the rake face. The quantitative presentation of flank wear and crater wear with cutting

distance is in Figure 5.19. The rake wear presented here is approximated by measurement of the wear area using Nomarski microscope. Figure 5.19 shows the amount of rake and flank wear with cutting distance. It is clear from the graph that the flank wear is very small but increased with the increase of cutting distance. In case of rake face, the wear is rapidly increasing with cutting distance.

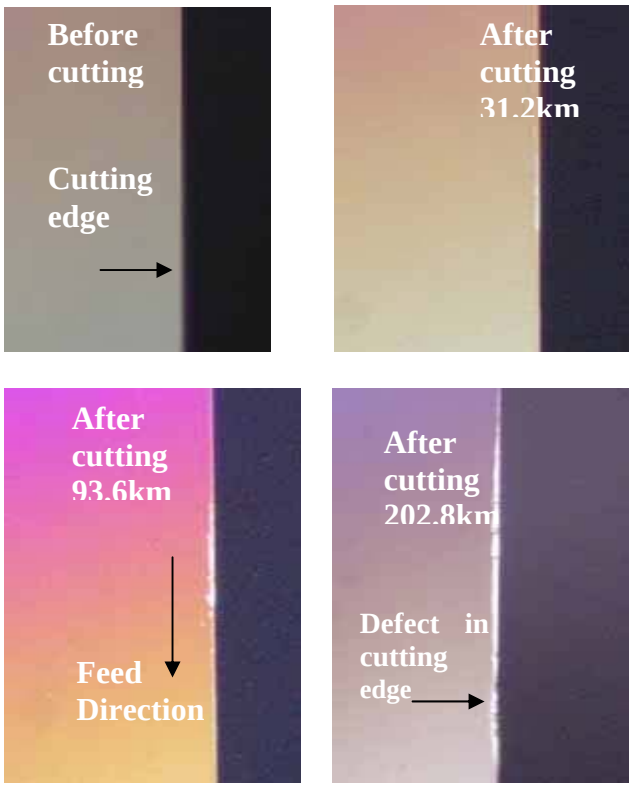

Figure 5.11: Flank wear of natural diamond cutter at different cutting distance

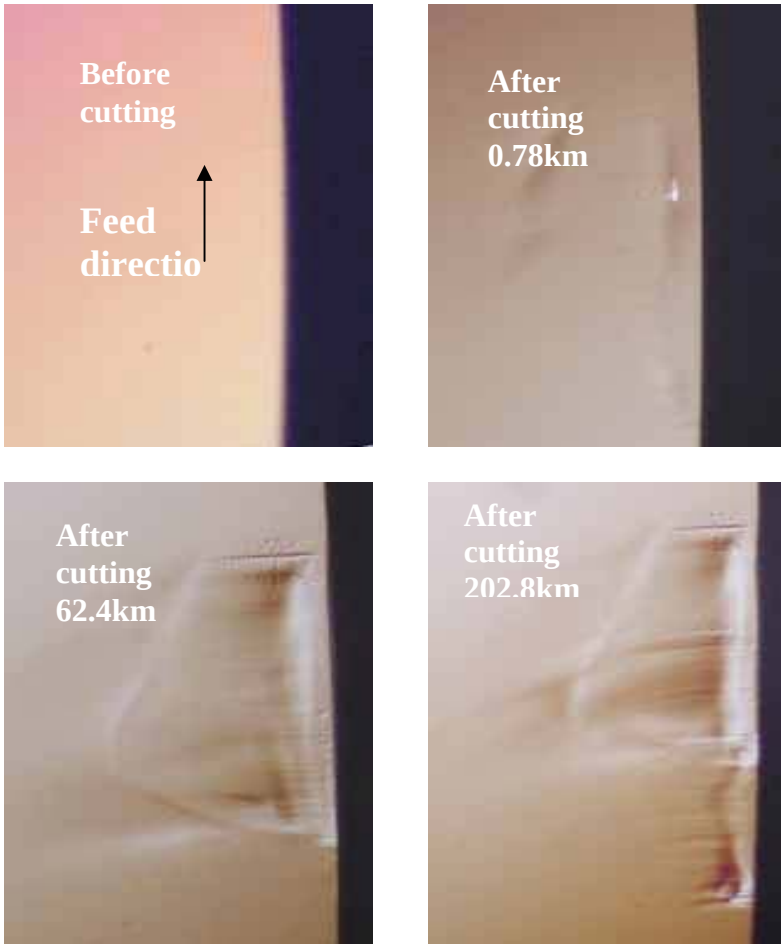

Figure 5.12: Rake wear of natural diamond cutter at different cutting distance.

5.3.1.2 Artificial diamond

The progression of tool wear of artificial diamond with cutting distance can be seen from Figure 5.13 & Figure 5.14 and graph in Figure 5.19. It is clear from the pictures that the nature of wear formation of artificial diamond tool is similar to that of natural diamond tool. The flank wear has increased with the cutting distance and rapid crater wear was observed up to certain cutting distance (75km) but after that the rate of wear increase tapered off.

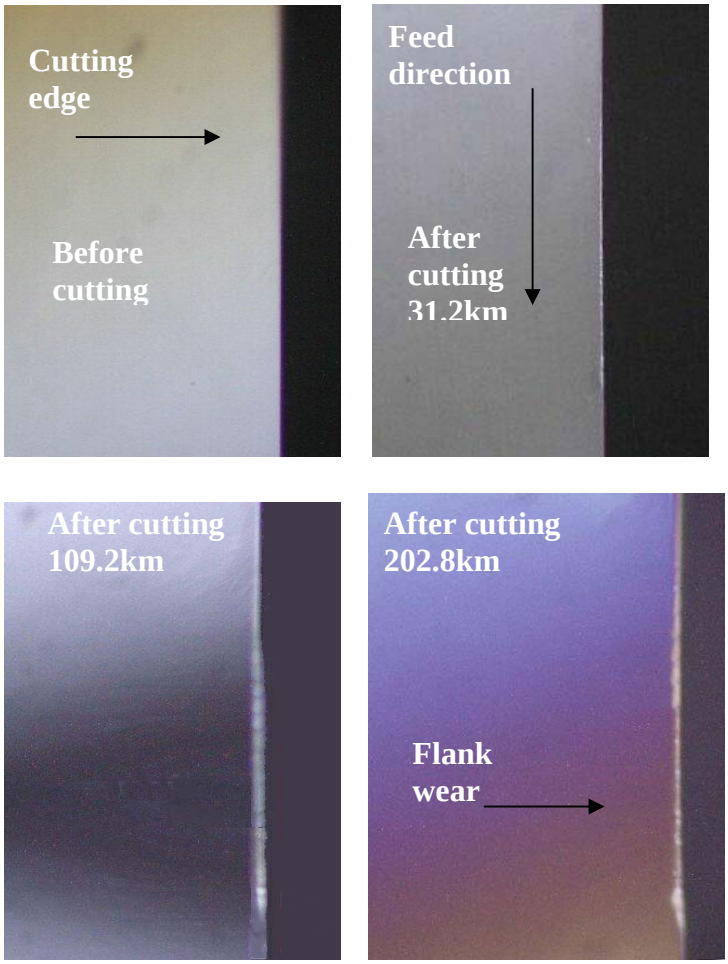

Figure 5.13: Flank wear of artificial diamond cutter at different cutting distance

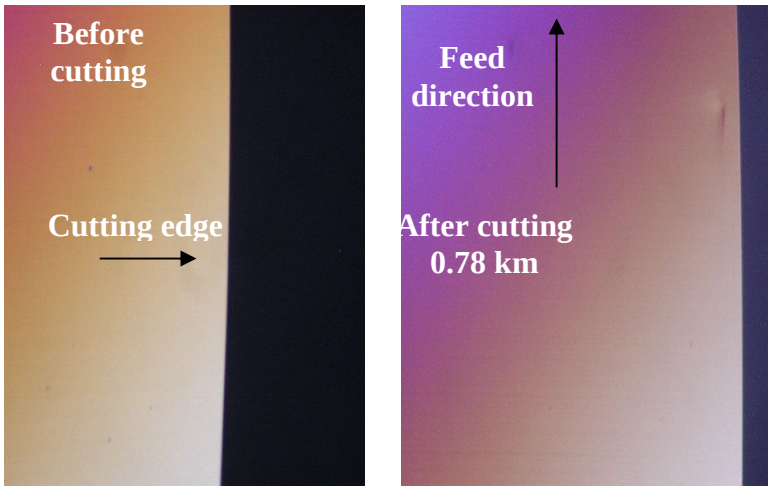

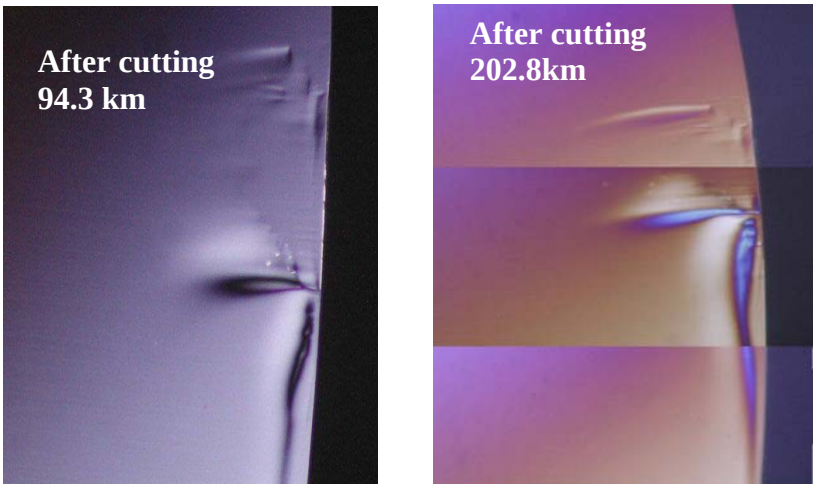

Figure 5.14: Rake wear of artificial diamond cutter at different cutting distance

5.3.2 SURFACE ROUGHNESS

5.3.2.1 Natural diamond

The appearance of machined surface at different cutting distance for natural diamond cutter can be seen in Figure 5.15. The tool feed marks on the surface changed with cutting distance as the wear developed at the tool's cutting edge. This change may be because of the position and depth of wear (grooves) at the flank face of the cutter. The surface roughness (R_a & R_y) of the machined surface has increased in very much random manner. The variation of surface roughness (Ra & Ry) of the machined surface with cutting distance is shown in Figure 5.20. It shows an increasing trend though not smooth one. This is due to the effect of very irregular development of wear at the rake face and the flank face of the cutting tool during machining.

Figure 5.15: Surfaces machined by natural diamond cutter at different cutting distance.

5.3.2.2 Artificial diamond

The appearance of machined surface at different cutting distance for artificial diamond tool is presented in Figure 5.16. Like natural diamond cutter, artificial diamond tool also produced surfaces with changing feed marks pattern. The variation of surface roughness with cutting distance is shown in Figure 5.20. The surface roughness has increased in a random manner like the other machined surfaces. It can be seen that the variation of R_a & R_y with cutting distance is quite similar to that of natural diamond cutter.

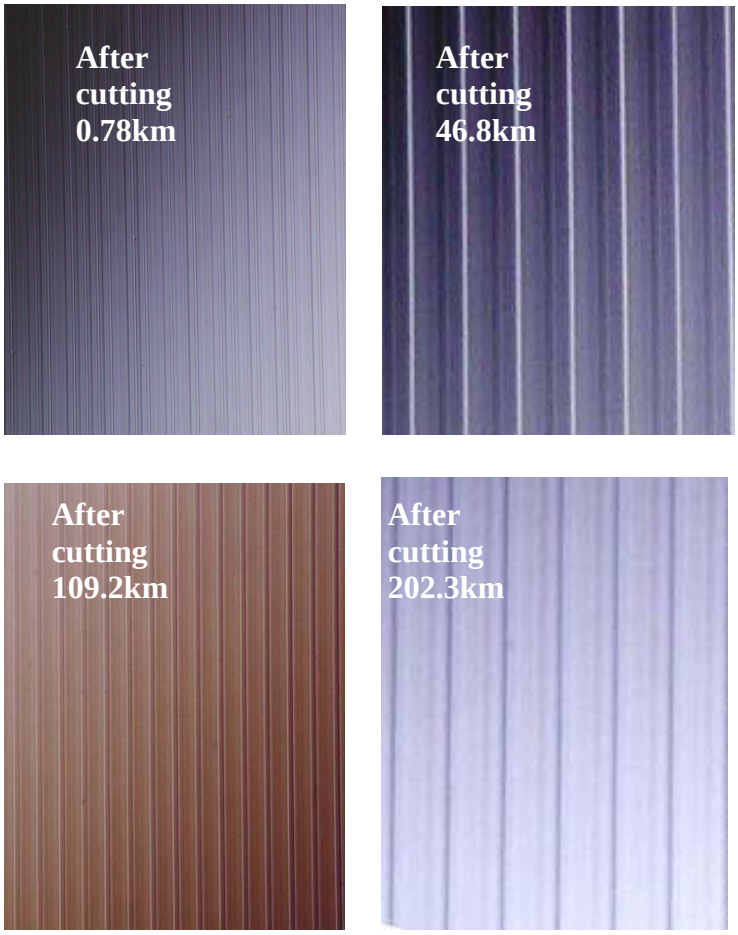

Figure 5.16: Surfaces machined by artificial diamond cutter at different cutting distance

5.3.3 CUTTING FORCES

The variation of cutting forces with cutting distance exhibits very interesting pattern. For artificial and natural diamond cutters, cutting force is generally higher than thrust force, and these forces show an increasing trend with cutting distance though not in smooth manner. For natural diamond cutter the thrust force graph crossed the cutting force graph after cutting around 160km as shown in the Figure 5.17a. This crossing of cutting force line by thrust force line has never happened in cutting 200km for artificial diamond (Figure 5.17b) but the difference between cutting force and thrust force have

decreased with the increase of cutting distance. This change of force is due to the formation of negative rake angle on cutter because of wear development.

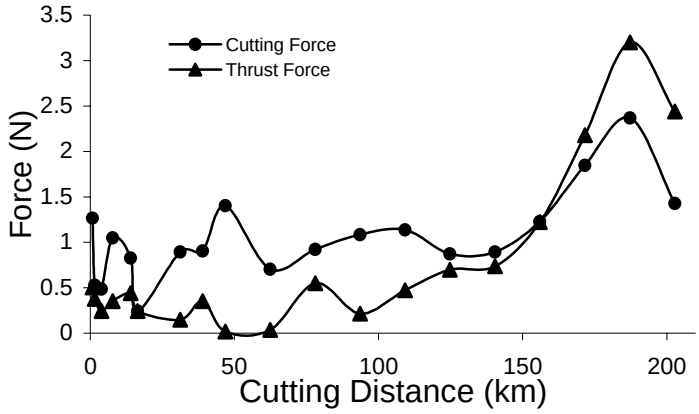

(a) Natural diamond cutter

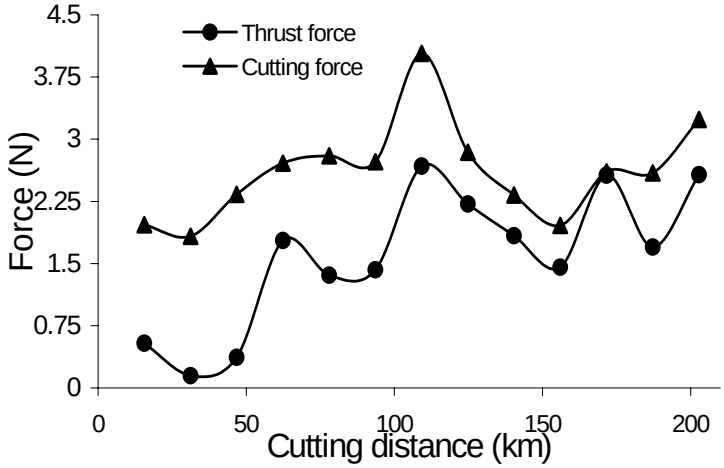

(b) Artificial diamond cutter

Figure 5.17: Effect of cutting distance on forces.

With the increase of cutting distance the cutting edge radius may have increased because of wear and this increased cutting edge radius creates negative rake which makes the thrust force higher as described in the Fig. 5.18. The Figure 5.18a shows the

cutting geometry at the start of cutting and 5.18b shows the cutting geometry after cutting 110km where F_t and F_c are thrust force and cutting force respectively.

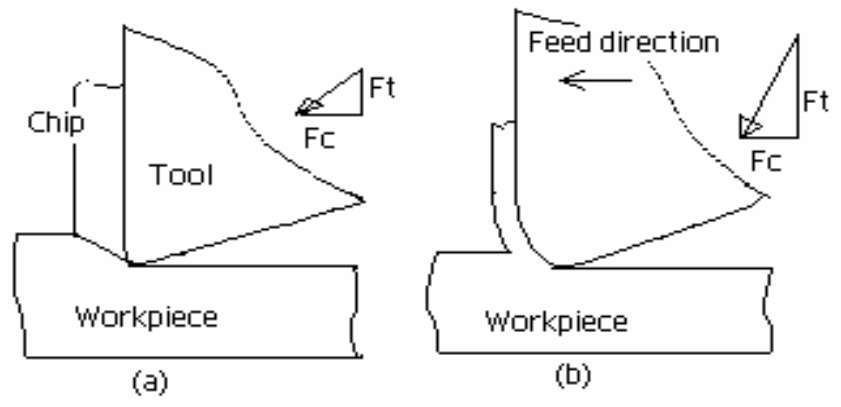

Figure 5.18: Effect edge radius on cutting mechanism

5.3.4 COMPARISON OF CUTTING PERFORMANCE

The Figures 5.19, 5.20, and 5.21 show the performance of artificial and natural diamond cutters in terms of wear, surface roughness and cutting forces respectively. It can be seen that least tool wear (crater and rake) occurred in the natural diamond cutter. Significant crater wear is apparent in artificial diamond cutter in comparison to natural diamond cutter (Figure 5.19) but both of the cutters experienced nearly the same pattern of flank wear development (Figure 5.19) with same trend in wear progression. Tremendous increase of crater wear was observed for both the cutters at the first few kilometers, after which the wear rate started to reduce and stabilize. The rapid wear rate was noted for up to 75km for artificial diamond cutter and 10km for natural diamond cutter. The performance of cuter in terms of surface roughness (R_a, R_y) seems very much similar (Figure 5.19), as both the cutters have given similar

surface finishes. In the case of machining force, it is clear that cutting force and thrust force are significantly lower for the natural diamond cutter compared to that of the artificial one. The differences in cutting forces is due to the difference in sharpness of the cutters in the start of cutting and, wear in the end of cutting.

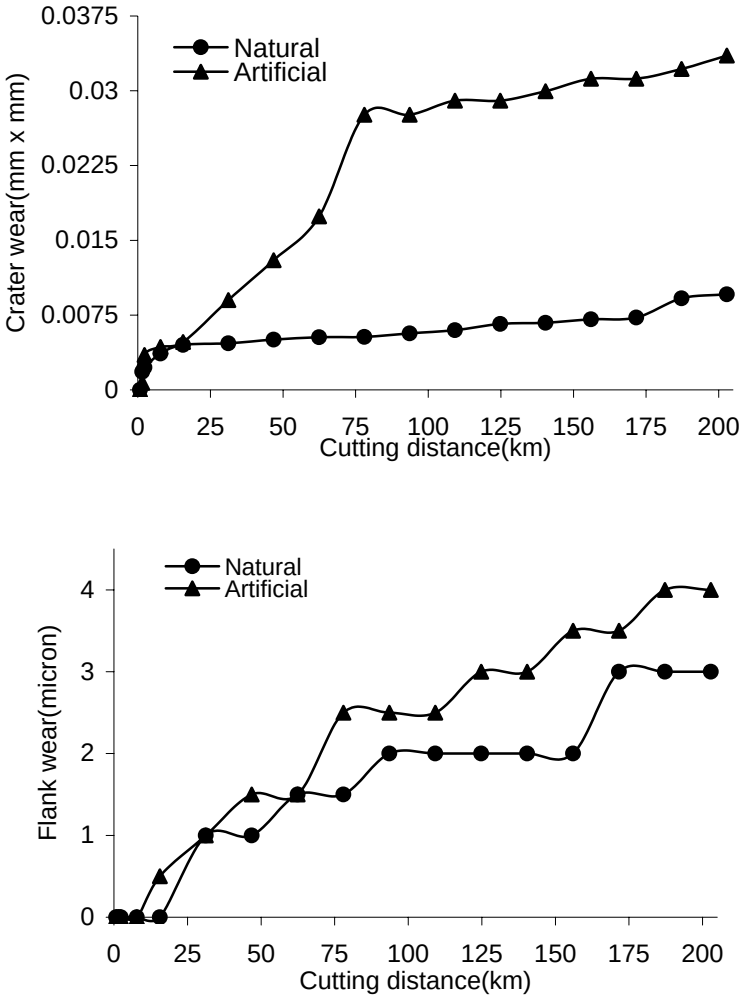

Figure 5.19: Effect of cutting distance on crater wear and flank wear for different cutter

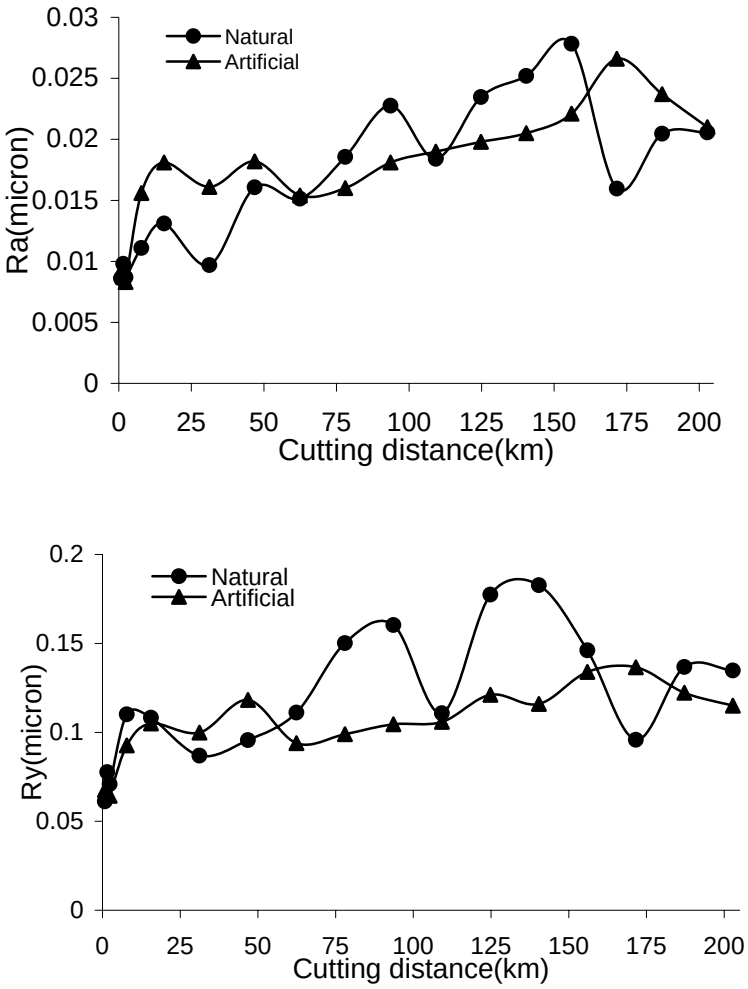

Figure 5.20: Effect of cutting distance on surface roughness (R_a and R_y) for different cutter

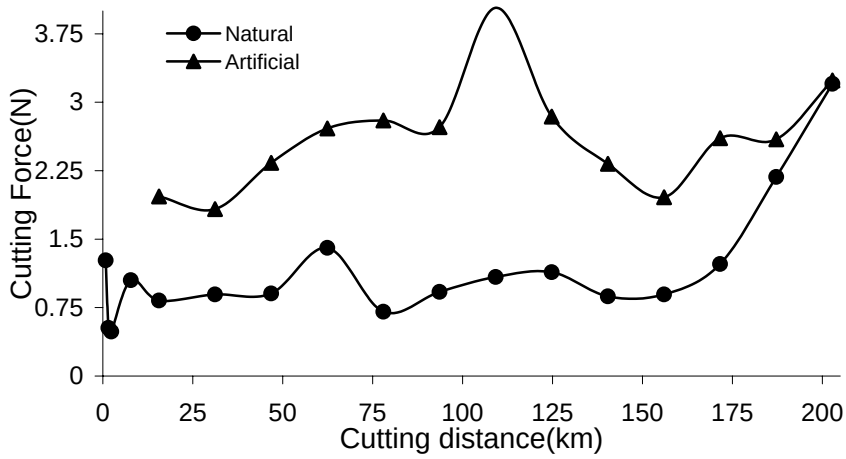

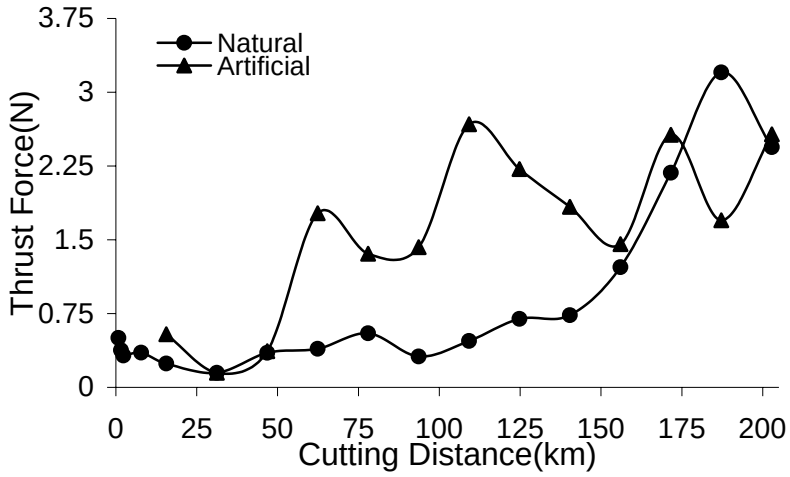

Figure 5.21: Effect of cutting distance on cutting force and thrust force for different cutter.

5.4 EFFECT OF PHOSPHORUS CONTENT ON THE PERFORMANCE OF ARTIFICIAL DIAMOND CUTTER

Workpiece material has great influence on cutting tool performance and phosphorus content influences the properties of electroless-nickel in a great extent. Phosphorus content mainly controls hardness and structure of electroless nickel [5]. So the effects of phosphorus content were experimented with two types workpieces of 5.8 % and 11.5 % (w/w) phosphorus. Tremendous and sever flank and rake wear were noticed for lower phosphorus content (5.8%w/w). From nomarsky picture the abrupt and irregular flank and rake wear were observed.

5.4.1 CUTTING TOOL AND MACHINED SURFACE

5.4.1.1 Phosphorus content 5.7%

While cutting electroless nickel of phosphorus contents 5.7 % (w/w) severe cutting tool wear was observed in the rake and flank face as in the Figure 5.22 and Figure 5.23. The nature of rake and flank wear is same but the grooves generated at flank face are very regular in comparison to the wear of rake face. The start of flank wear noticed at the very beginning of cutting i.e. after cutting 0.78km and rake wear started after cutting around 7.8km. The pictures of surface at Figure 5.24 show the change of surface appearance and this change of surface represents flank face profile of the cutter. A careful observation of surface shows that the surface profile consists of complete replica of cutter profile.

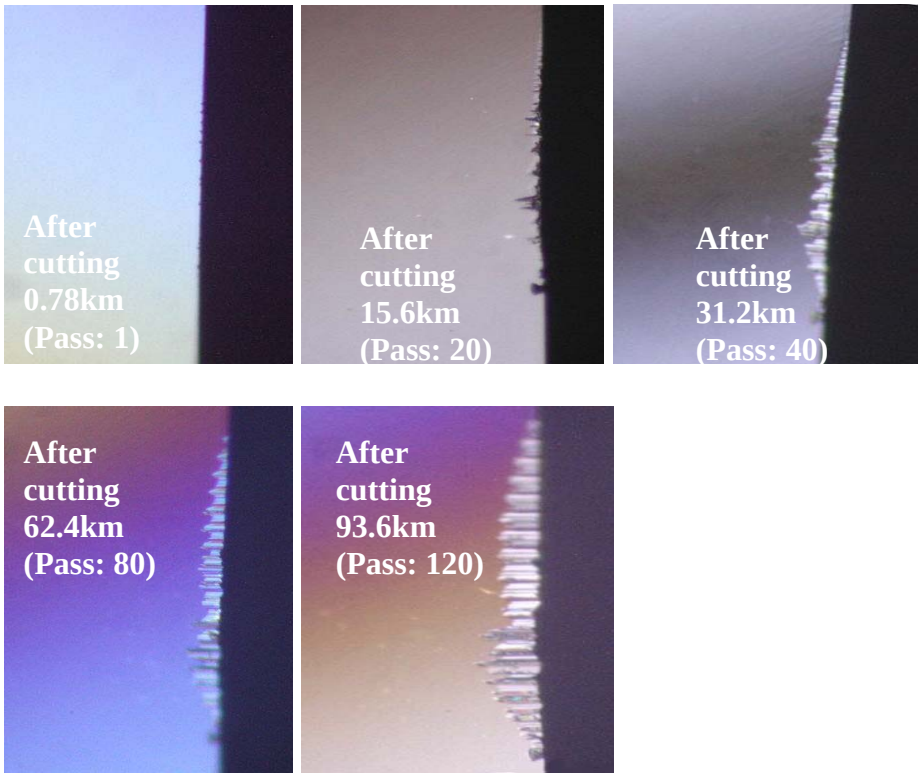

Figure 5.22: Flank face for cutting EN of %P (w/w)=5.7, at different cutting distance.

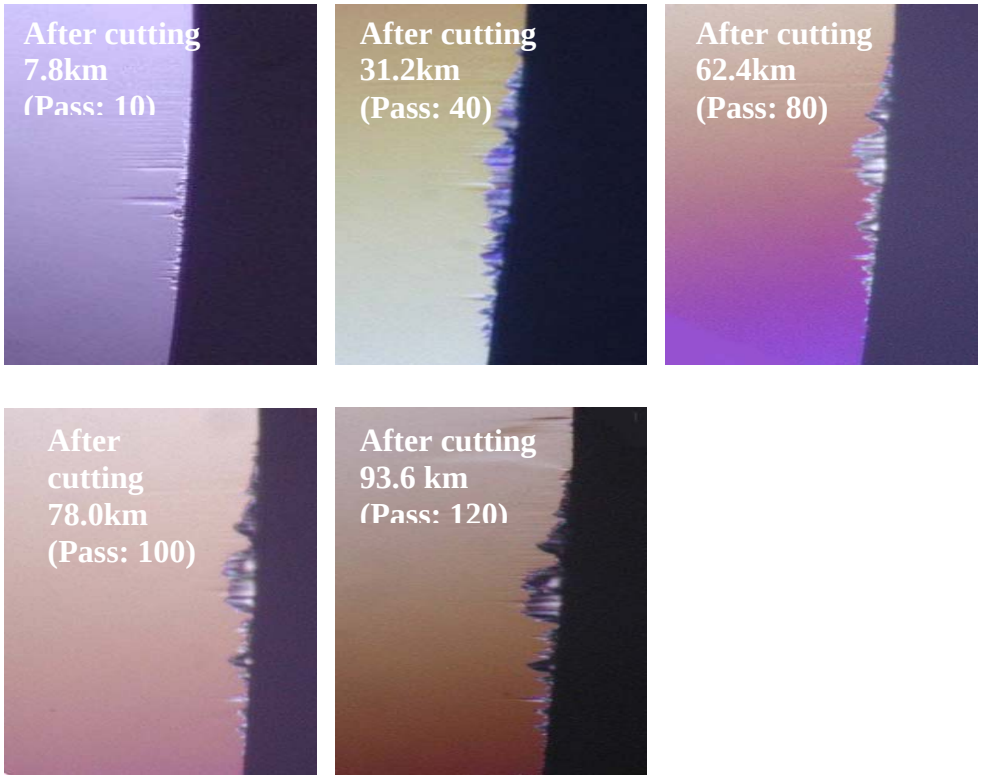

Figure 5.23: Rake face for cutting EN of %P (w/w)=5.7, at different cutting distance

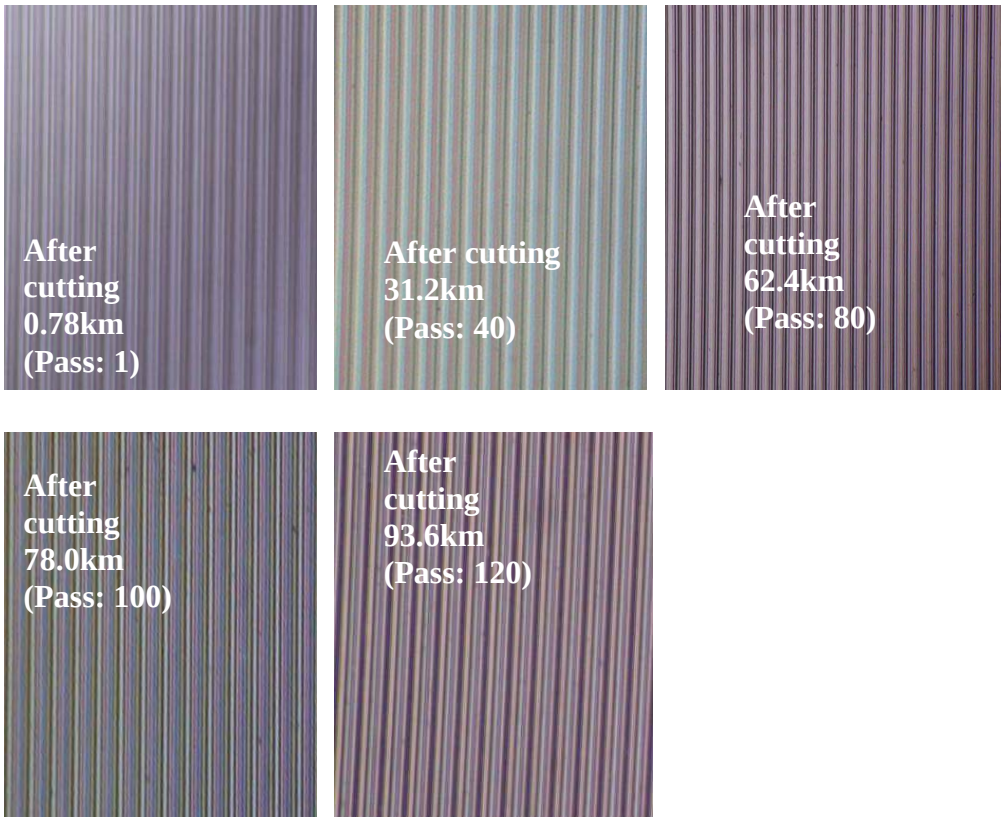

Figure 5.24: Surface for cutting EN of %P (w/w)=5.7, at different cutting distance

5.4.1.2 Phosphorus content 11.5%

Negligible wear was observed on rake and flank face during cutting electroless nickel with phosphorus content 11.5 % (w/w) as shown in the Figure 5.25 and Figure 5.26. Very thin grooves were noted in the flank face and a white line was appeared in the cutting edge at rake face. The appearance of machined surface (Figure 5.27) was changed with cutting distance but the surface of this time is much smoother than the surface of electroless nickel with phosphorus content 5.7 % (w/w). The difference in surface appearance between two types of phosphorus contents is because of different amount cutting tool wear. The pictures of surface and cutting tools show the effect of phosphorus content on machining performance.

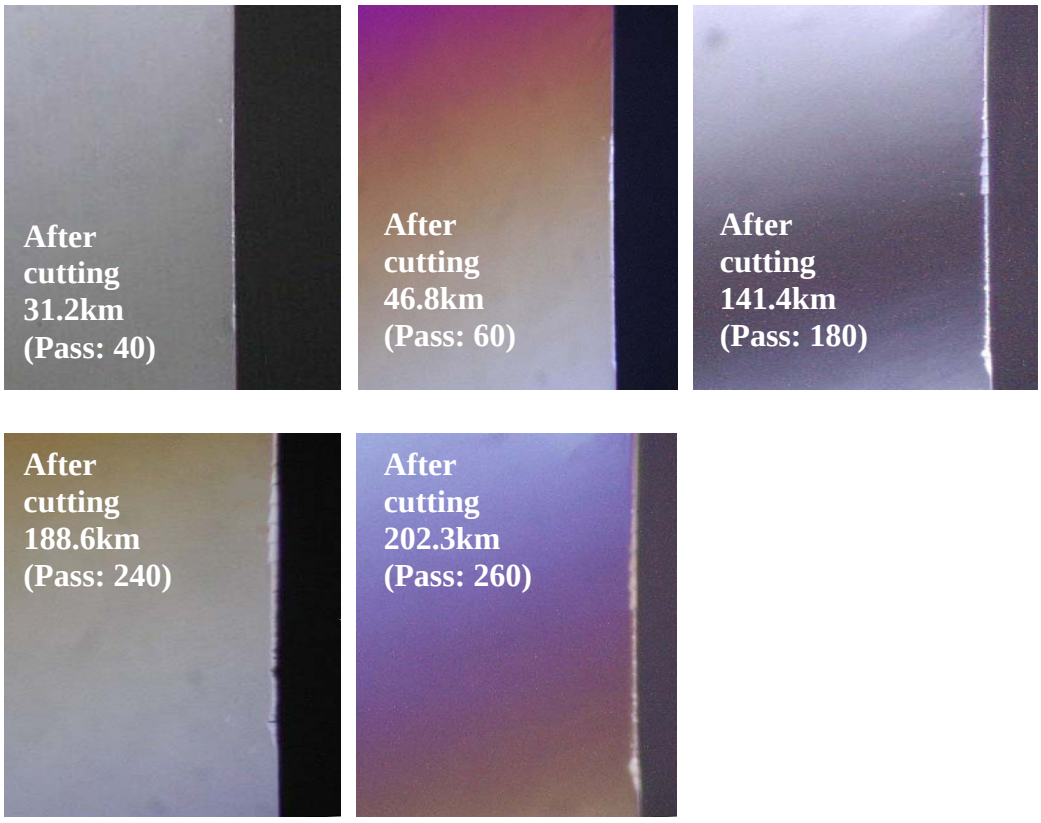

Figure 5.25: Flank face for cutting EN of %P (w/w)=11.5, at different cutting distance

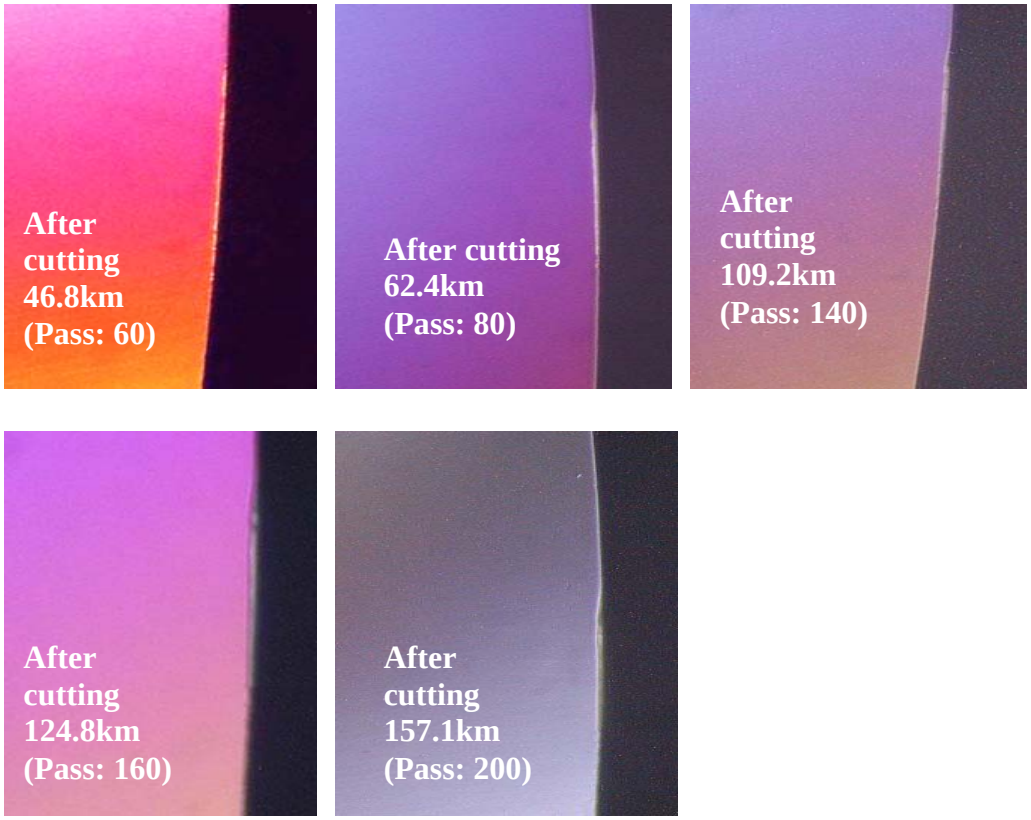

Figure 5.26: Rake face for cutting EN of %P (w/w)=11.5, at different cutting distance

Figure 5.27: Surface for cutting EN of %P (w/w)=11.5, at different cutting distance

5.4.2 COMPARISON OF CUTTER PERFORMANCE

The quantitative comparisons of cutting tool wear for different phosphorus content have been presented in the Figure 5.28. From the figure it is very clear that rate of flank and rake wear is very small and almost constant for 11.5 % (w/w) phosphorus content. On the other hand tool wear was of so high rate that machining had to be stopped after cutting around 100km for electroless nickel with lower phosphorus content. Primarily phosphorus plays three main roles i.e. controls hardness, material structure and lubricates the machining process of electroless nickel. Though Electroless nickel with lower phosphorus content is harder and brittle, no brittle fracture was noticed during machining. So it seems that phosphorus content plays some more roles in chemical property of electroless nickel and tool wear. It is clear that phosphorus protects the cutter from damage and facilitates the machinability of electroless nickel. The effect of cutting distance on surface roughness (R_a and R_y) has been shown in the Figure 5.29, a significant difference in surface roughness in terms of R_a is clear but R_y is not indicating any significant difference between two surfaces.

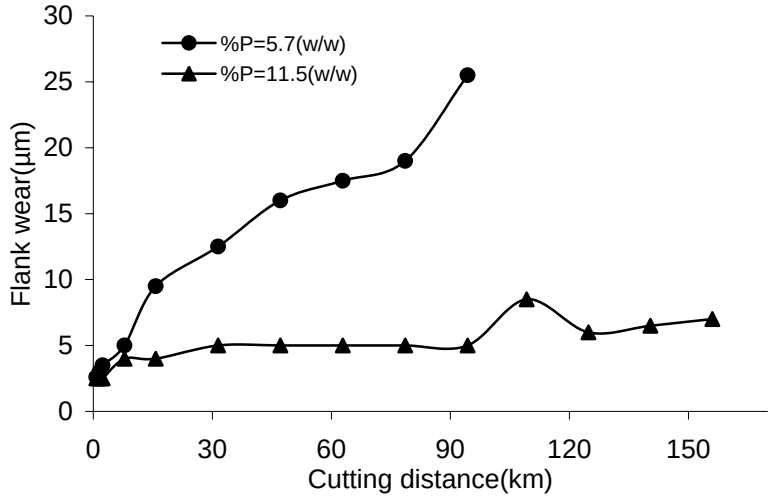

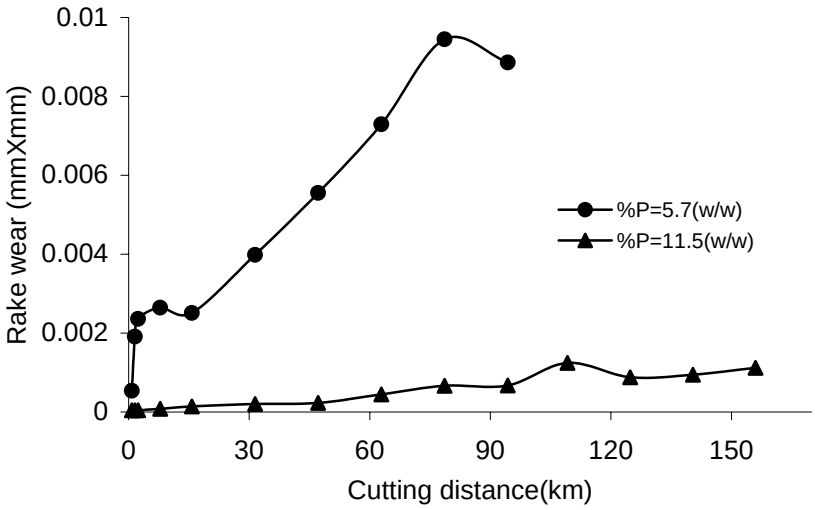

Figure 5.28: Effect of cutting distance on crater wear and flank wear for different phosphorus content.

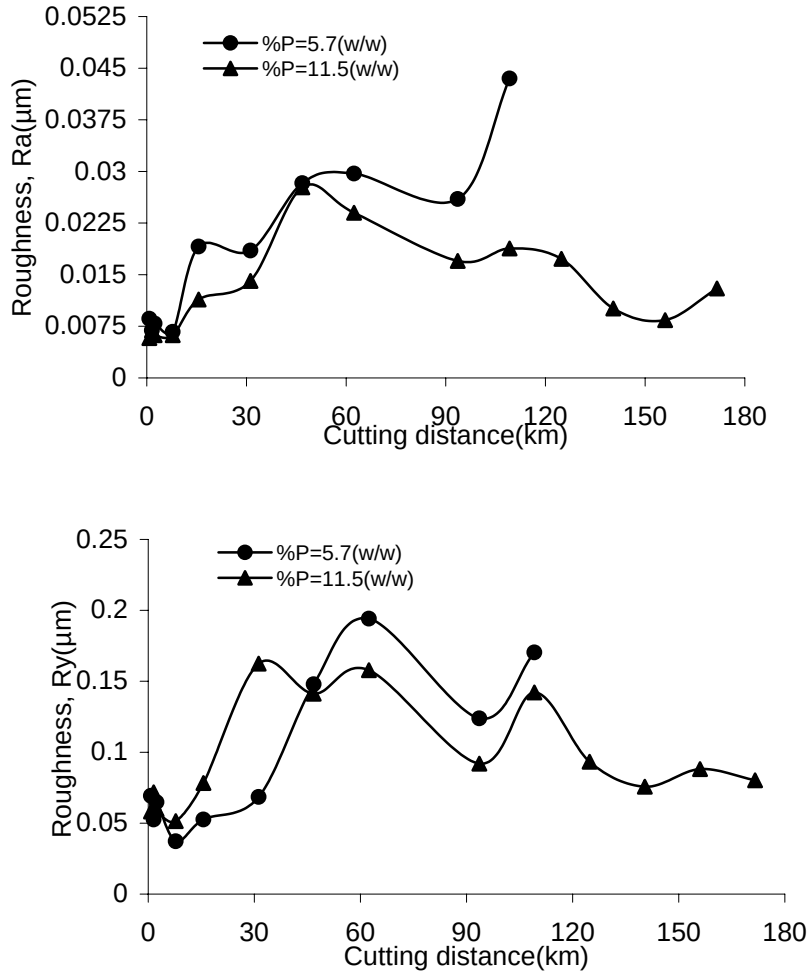

Figure 5.29: Effect of cutting distance on surface roughness with different phosphorus.

5.5 EFFECTS OF DEPTH-OF-CUT ON ARTIFICIAL DIAMOND CUTTER PERFORMANCE

For any machining process the selection of depth-of-cut has great effect on cost reduction, machining performance, inventory management etc. This section of the thesis investigates the effects of depth-of-cut in case of ultra-precision machining of electroless-nickel.

5.5.1 4µm depth of cut

Figure 5.30 and Figure 5.31 shows the pictures of flank face and rake face at different cutting distance respectively. The cutter was used to cut the electroless nickel with around 10 % (w/w) phosphorus content. The wear occurred uniformly in the grooved form. Some wear had appeared at rake face and flank face and spread to some extent with a sequence of repeated cutting, for total cutting distance of 202km. The possible wear progression process at rake face can be seen in Figure 5.31. It is clear from the picture that the defect arose at rake face after cutting 7.8km and the wear developed clear shape after cutting 80km and after this the defective zone was nearly unchanged up to 202.8km cutting distance. This type of wear at rake face is quite interesting which is difficult to classify. The EDX analysis showed no material deposition at rake face and it is not possible to get a complete surface topography of the wear zone as the area is too large for the AFM (Atomic Force Microscope) and too small for telystep stylus profiler. The causes and nature of this type of wear are under investigation. In case of the flank face some wear appeared after cutting 15.6km as a bright line through the cutting edge at flank face, which was not detectable by SEM. Some groves spaced at 10µm were also noticed across the bright line of cutting edge. This type of wear may

be termed as wear of stepped form. Uncut portion of workpiece due to worn cutting edge causes the growth of stepped wear in the following manner. As the cutting distance increases, a portion of cutting edge is worn out and the uncut or low depth of cut potion arise on the workpiece. This portion of workpiece is then removed by adjacent cutting edge, thus a secondary wear zone is created. The width of material removal is identical as feedrate is same but depth of cut for first wear zone is higher than that of second wear zone [34]. With the increase of cutting distance groves were more evident. The pattern of wear progression is shown by the picture sequence of Figure 5.30.

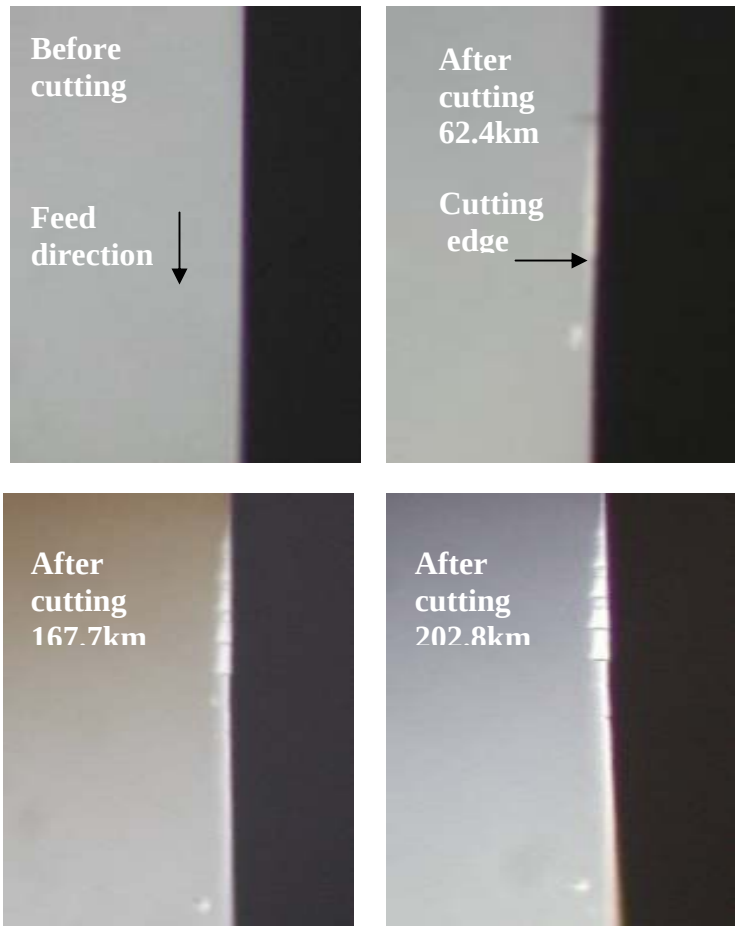

Figure 5.30: Stages of flank wear at different cutting distance form Nomarski.

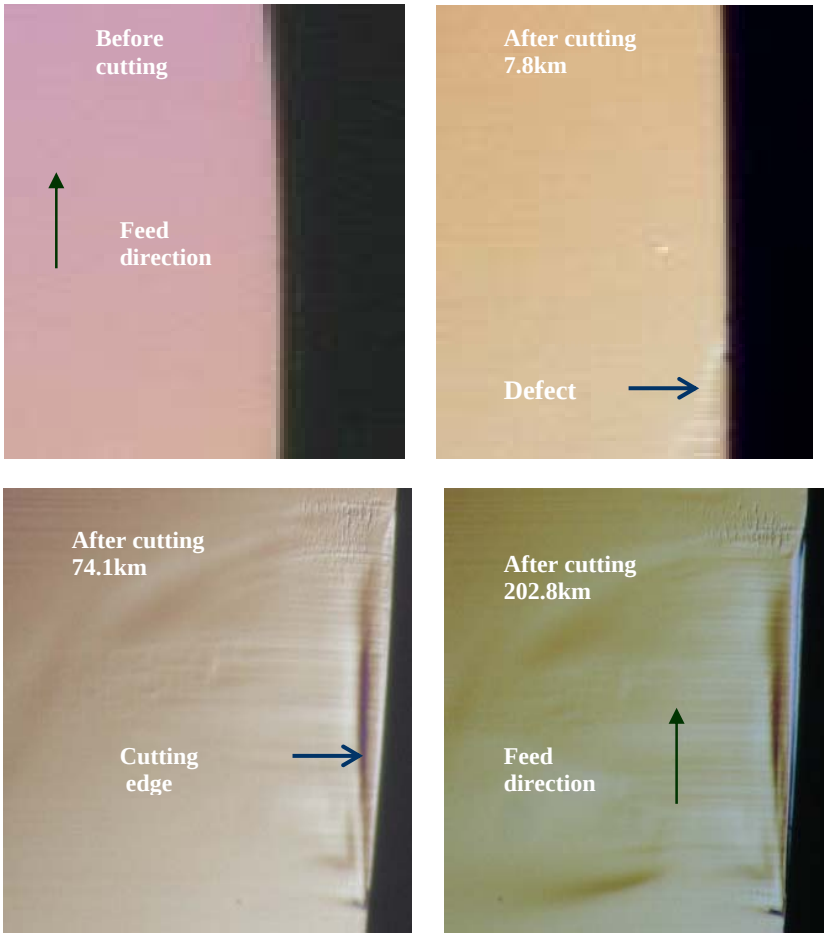

Figure 5.31: Stages of crater wear at different cutting distance form Nomarski .

5.5.2. 2µm depth of cut

While turning electroless-nickel with the depth-of-cut 2µm the appearance of flank face and rake face with cutting distance can be presented by Figures 5.31 & 5.32 respectively. It seems that nature of wear development is very similar to that of cutting tool during cutting with depth-of-cut 4µm. But the groove at flank face was not so distinct and merged to each other. The wear at rake face is difficult to describe.

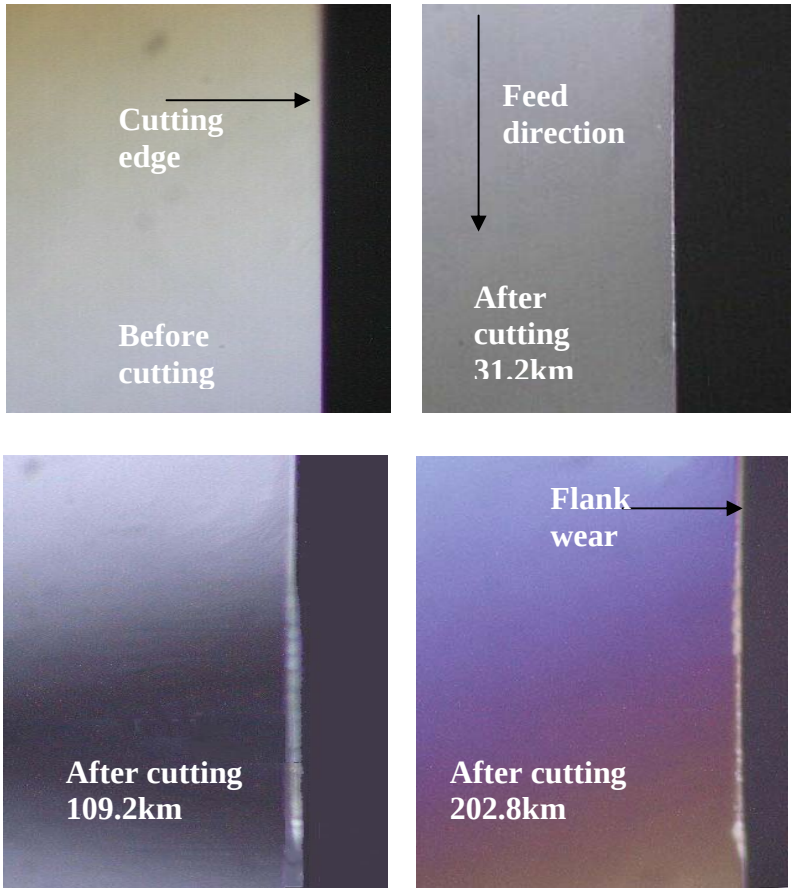

Figure 5.32: Stages of flank wear at different cutting distance form Nomarski.

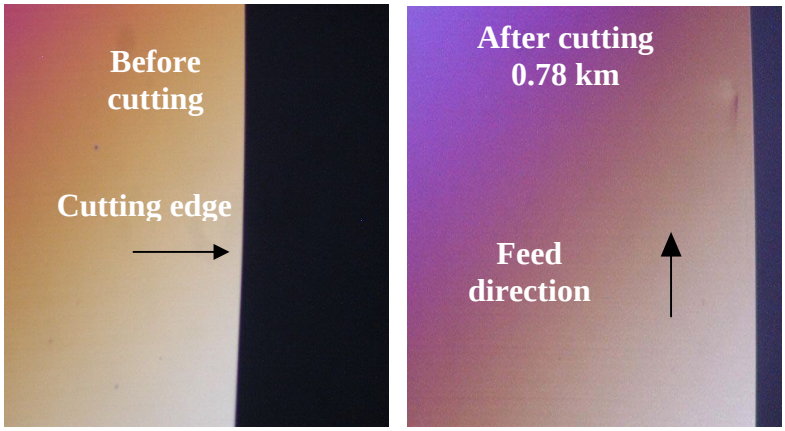

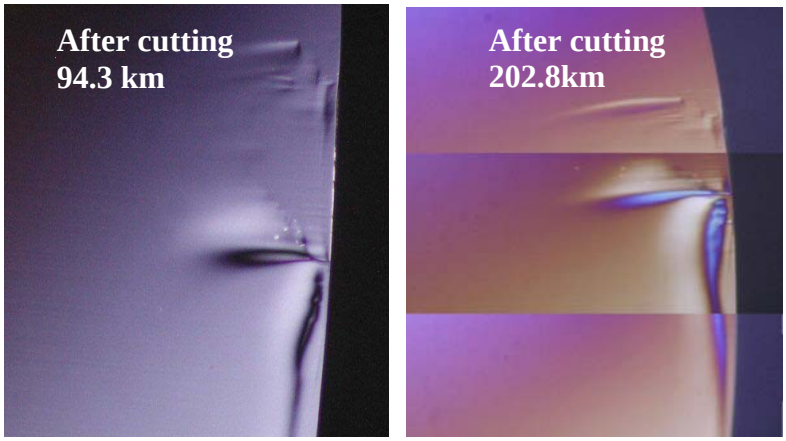

Figure 5.33: Stages of rake wear at different cutting distance form Nomarski.

5.5.3 Surface for different depth-of-cuts

The appearances of surface at different cutting distances with 4µm depth-of-cut and 2µm depth-of-cut have been presented in the Figure 5.34 and 5.35 respectively. For both of the time the cutting edge profiles on the machined surface have been changed with cutting distance because of the wear at rake and flank face. A careful observation of surfaces for different depth-of-cut does not give any significant conclusion about the effect of depth-of-cut on surface appearance.

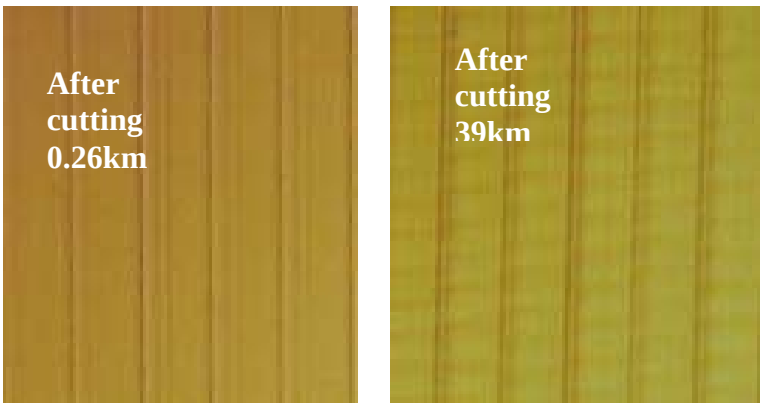

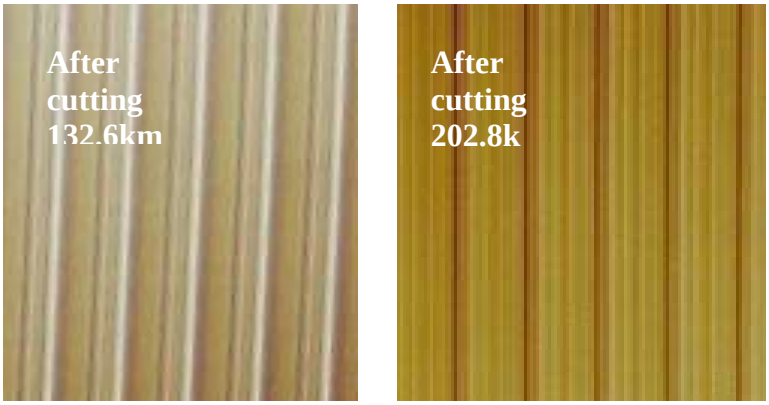

Figure 5.35: Appearance of surface at different cutting distance with 4µm depth-of-cut

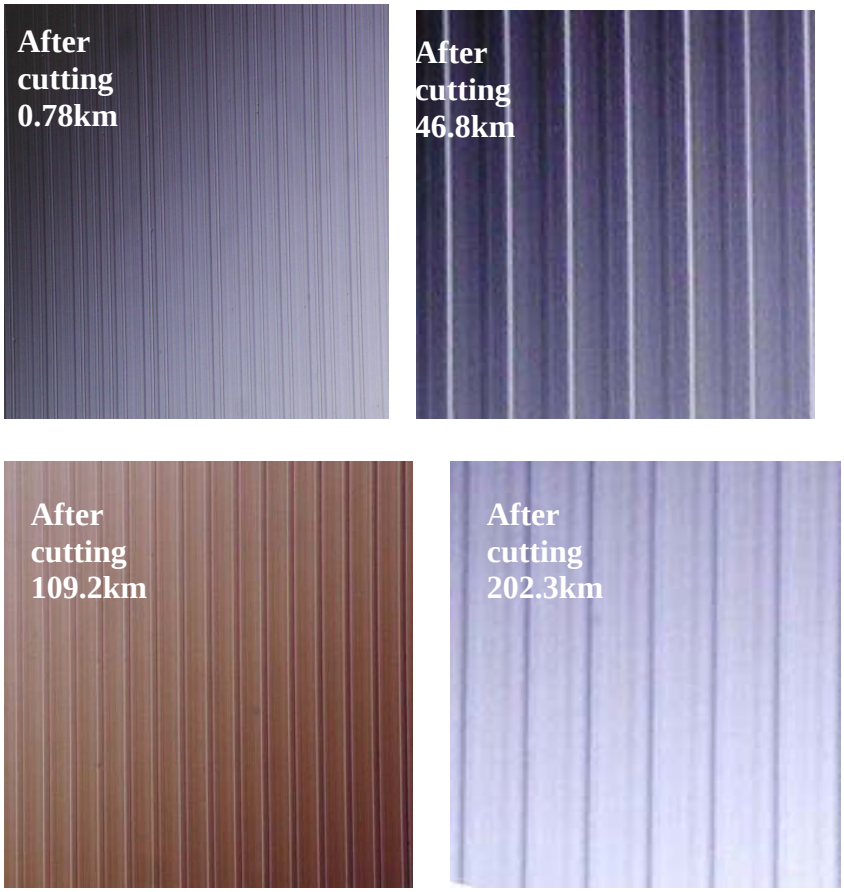

Figure 5.36: Appearance of surface at different cutting distance with 2µm depth-of-cut

5.5.4 Comparison for different depth-of-cut

A clear idea can be obtained about the quantitative rake and flank wear from the Figure 5.37. The overall flank wear is little bit higher for 2µm depth-of-cut than that of 4µm depth-of-cut. In case of rake the wear for 2µm depth-of-cut is much higher than that of 4µm depth-of-cut. Very high wear rate was noticed for 2µm depth-of-cut up to 80km of cutting distance after that the wear was not spread so much. For 4µm depth-of-cut high wear rate was noticed during cutting of 80km to 110km. Four types of wear for diamond tool is well established i.e. mechanical attrition, fracture, thermal degradation and chemical wear [35]. For this project the chemical affinity between high phosphorus contained workpiece and cutter is very low or absent so the total tool wear is the result of mechanical attrition, fracture and thermal degradation. The mechanical attrition, fracture and thermal degradation of the cutter are dominated by specific energy or stress applied during machining and specific cutting energy increases with the decrease of depth-of-cut or undeformed chip thickness [27]. This might be the one reason for increased cutting tool wear with lower depth-of-cut.

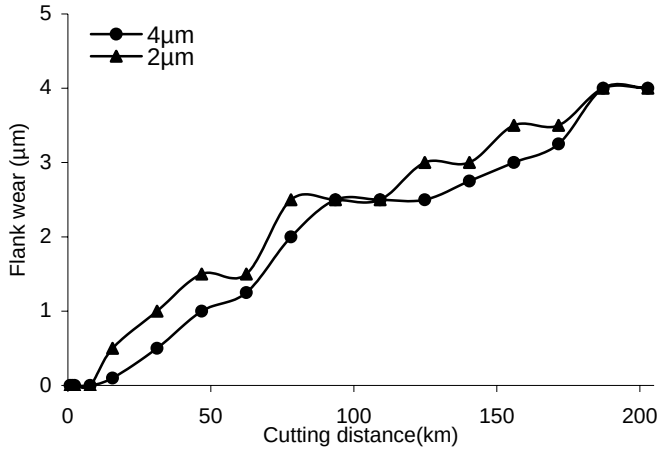

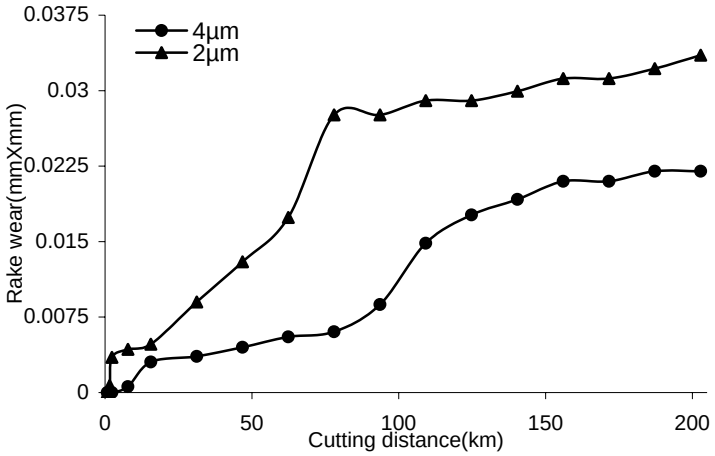

Figure5.37: Effect of cutting distance on tool wear for different depth-of-cut

The effect of cutting distance on surface roughness for different depth-of-cut is shown in the Figure 5.38, where surface roughness increases with the increase of cutting distance. Though cutter wear for 2µm dept-of-cut is higher than that of 4µm dept-of-cut but in terms of surface roughness it is difficult to identify any significant effect of depth-of-cut on surface roughness.

The Figure 5.39 presents the effect of cutting distance on forces for different depth-of-cuts. All the forces for both of the depth-of-cuts were very irregular and almost constant all over the cutting distance of 200km except the thrust force for 4µm dept-of-cut where tremendous increase of force was observed after cutting around 100km.

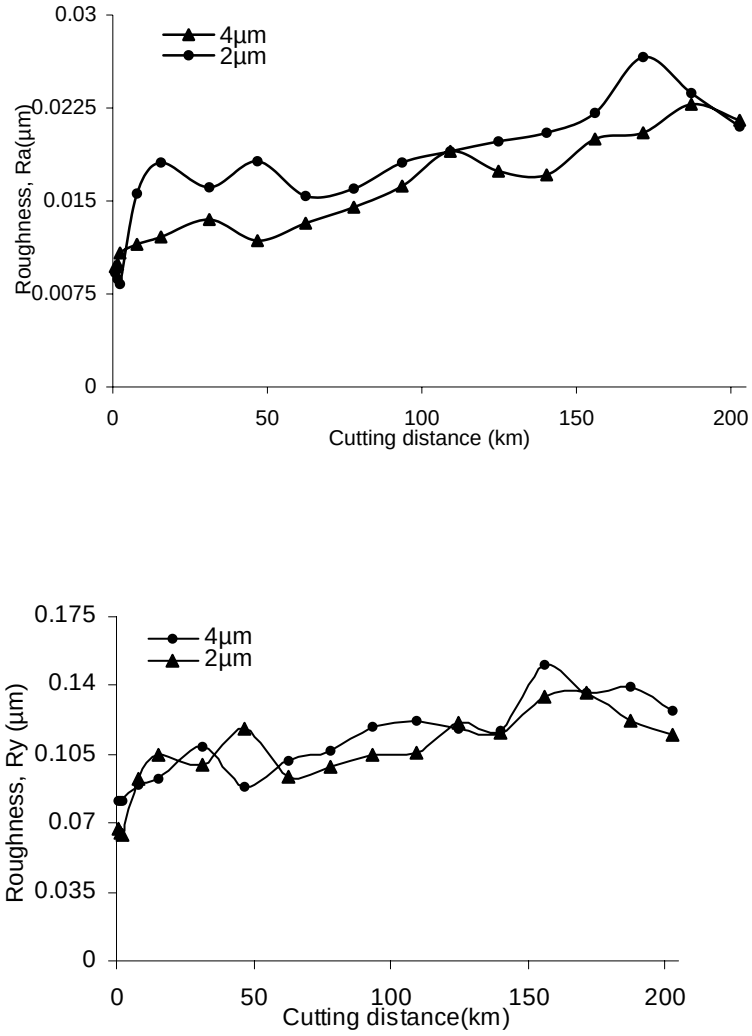

Figure 5.38: Effect of cutting distance on surface roughness for different depth-of-cuts

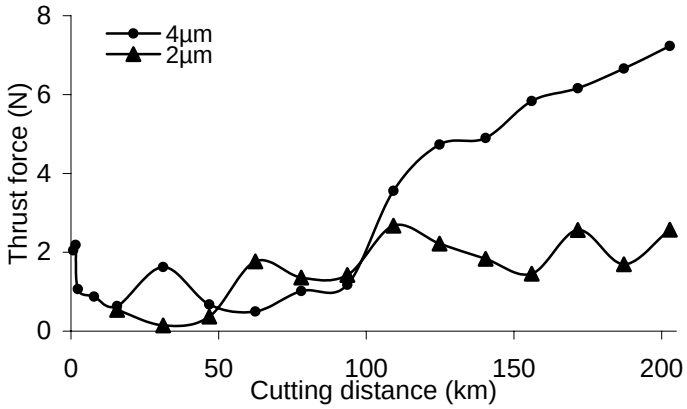

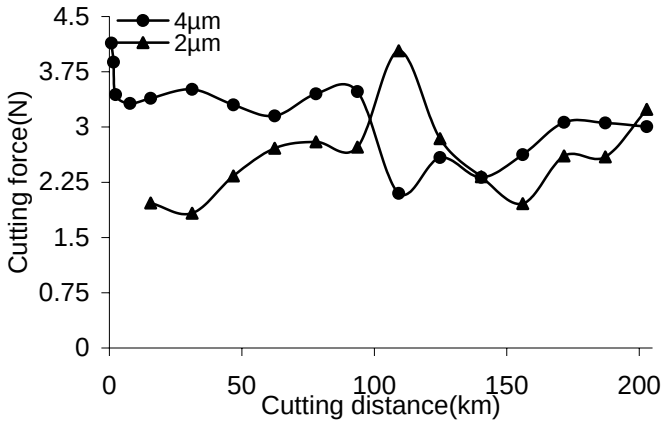

Figure 5.39: Effect of cutting distance on forces for different depth-of-cuts

5.6 CONCLUSION

This is the main chapter of the whole work. All the essential and presentable experimental data have been described sequentially.

6

CONCLUSIONS AND RECOMMENDATIONS

6.1 CONCLUSIONS

This investigation is an attempt to understand the prospects of ultra-precision machining of electroless-nickel plated die material. The main attention was given to the optimization of machining conditions to achieve minimum surface roughness and tool wear characteristics for different cutting tools, different workpiece compositions and different depth-of-cut for very long cutting distance. From the experimental results and discussions the following conclusions can be drawn:

1) Surface roughness of electroless-nickel (phosphorus content 9.59 percent w/w) is not affected significantly by variation of depth-of-cut (2µm-10µm). Surface roughness increases proportionally with the increase of feed rate. There is a critical value of spindle speed at which best surface finish is achieved. Higher phosphorus content gives better surface finish. Cutting force and thrust force increase with increase in depth of cut, spindle speed and feed rate but decrease with increase in phosphorus content.
2) Significant difference in surface appearance was noticed only with changing feederate. However, other factors did not affect the surface appearance significantly in the range of the experiments.
3) It is noted that for very long cutting distance the pattern of flank wear and rake wear development is the same for both artificial and natural diamond cutters as observed under Nomarski microscope. However, the amount of wear is different. In terms of the rake face tool wear, artificial diamond cutter experienced a much

larger crater wear compared to the natural diamond cutter. The progression of flank wear with cutting distance seems to be small for both cutters, but results still show that the natural diamond cutter experiences less flank wear compared to the artificial one.

4) Cutting force data show that the natural diamond cutter experienced lower cutting and thrust forces than the artificial one. This can best be explained by the sharper cutting edge at the beginning of the cutting test and lower wear rate of the natural diamond cutter at the end of the cutting test.
5) In terms of surface roughness, natural diamond performs better as the increase in surface roughness with cutting distance for natural diamond cutter was more stable than that for artificial diamond. For both cutters, surface roughness increased with cutting distance but after cutting for 200km, the surface finish achievable was still a mirror finish for both cutters.
6) The study to compare artificial and natural diamond cutter shows that the natural diamond cutter is able to perform better than the artificial diamond cutter. However, from the perspective of cost, the natural diamond cutter is 3-4 times costlier than the artificial one. Hence, comparison of the cost-benefit of the artificial and natural diamond cutters would have to be worked out based on application requirements.
7) The phosphorus content of electroless-nickel is the key factor for determining the machinability of electroless-nickel. Very high wear rate was noticed for electroless-nickel with less phosphorus content. Better surface appearance and surface finish were achieved for electroless-nickel with higher phosphorus content. Because for higher phosphorus content, tool wear is less and the workpiece is more ductile.

8) Depth-of-cut plays a significant role only in tool wear. Higher cutting tool wear was observed for low depth-of-cut.

6.2 RECOMMENDATIONS

1) All the cutting parameters used here for optimization should be extended to a greater extent, as the sensitivity for ultra-precision machining is very high, making it difficult to conclude about the optimum value for any machining parameters.
2) Some researchers have proved that the properties of diamond cutting tool, especially natural diamond cutter, are very uncertain and depend on many factors. So an intensive study should be performed to describe diamond cutters uniquely and compare them in terms of cost and performance for very long cutting distances.
3) A large extent of phosphorus content should be considered during experimentation to find the optimum percentage of phosphorus for best performance of cutter and machinability of electroless nickel.
4) Recently ultra-sonic vibration is being added to the cutting tool to improve surface finish for CNC machining. This method can be applied for ultra-precision machining and the performance of the machining can be compared.
5) A model for ultra-precision machining electroless nickel should be developed to minimize the cost for optimization of tool life, time and performance during mass production of machined products.
6) A new approach should be introduced to express and compare the actual diamond tool wear during machining because the tool wear observed in this project was difficult to express and compare in the conventional way. As SEM is not suitable for measuring tool wear of diamond cutter and the scope of measuring wear by

AFM (Atomic Force Microscope) is limited to only a certain area, a suitable machine needs to be developed for measuring diamond tool wear.

REFERENCES

[1] Nario Taniquechi. Current status in, and future trends of, ultraprecision machining and ultrafine materials processing, Annals of the CIRP Vol. 32/2/1983, pp573-582.

[2] T. Masuzawa. State of the art of micromachining, Annals of the CIRP Vol. 49/2/2000, pp473-488

[3] H. Weule, V. Huntrup, H. Tritschler. Micro-Cutting of steel to meet new requirements in miniaturization, Annals of the CIRP Vol. 50/1/2001, pp 61-64.

[4] G. M. Sanger, J. W. Dini. A perspective on electrodeposited and electrolee nickel coatings used in optical applications. In Proc SUR/FIN' 82, American Electroplaters and surface finishers society1982

[5] J. W. Dini, C. K. Syn, J. S. Taylor, G. L. Mara, R. R. Vandervoort and R. R. Donaldson. Influence of phosphorus content and heat treatment on the machinability of electroless nickel deposits. In Proc. Electroless Nickel conf.IV(Chicago), 1995, Gardner Publications, Cincinnati, pp5-1 to 5-15.

[6] James R. Henry. Electroless (autocatalytic) plating. Metal finishing. Guidebook & directory issue, Metals and Plastics Publications, 1980, Hackensac, NJ, pp.267-287.

[7] Md. Haider-e-Alahi. Rapid tools with improved surface finish and strength. Master degree thesis, National University of Singapore, 2000.

[8] *Electroless Nickel Plating-Wolfgang Riedel-1991*

[9] J. M. Casstevens and C. E. Daugherty. Diamond turning of surface on electroless nickel. in Precesion Machining of T. T. Saito,ed.,Proc. SPIE159, 109(1978)

[10] A. mayer, R. D Bramlett and R. D. Day. Electrodeposited coatings for diamond turning applications. Monterey, CA:OF&T, 1989.

[11] J. Wilks. Performance of diamonds as cutting tools for precision machining, Precision Engineering, V-2, P-57, 1980.

[12] Wolfgang Riedel, 'Electroless-nickel plating", Published by ASM international, pp206, Metals Park, Ohio, U.S.A, 1991.

[13] Syn, C. K., Taylor, J. S., Donaldson, R. R. Diamond tool wear Vs cutting distance on electroless nickel mirrors, Proc. SPIE, Vol 676, pp128-140, 1986.

[14] J. M. Oomen, J. Esses. Wear of monocrystaline diamond tools during ultra-precision machining of non ferrous metal, Precision Engineering,Vol-14,No.4, pp206-218, 1992.

[15] A. Bhattacharyya. Metal Cutting Theory and Practice. Calcutta, India, New Central Book Agency, pp126, 2000.

[16] David K. Felbeck, Anthony G. Atkins. Strength and Fracture of Engineering Solids. Second edition, New Jersy, USA, pp 308-343

[17] George E. Dieter. Mechanical Metallurgy- SI Metric edition. McGraw-Hill Book Company, Singapore, 2001.

[18] Dominique P. Miannay. Fracture Mechanics. Chapter 5, Springer,

[19] Liu Kui. Ductile Cutting For Rapid Prototyping of Tungsten Carbide Tools. PhD Thesis, National University of Singapore, Singapore, 2002.

[20] A. Muchtar. Fracture properties of fine-grained high purity alumina. Master degree thesis, National University of Singapore, pp 62, 1998.

[21] Chan yuen yin. Shaping of alumina ceramics. Master degree thesis, National University of Singapore, pp 21, 1999.

[22] Z.J. Yuan, M. Zhou, S. Dong. Effect of diamond tool sharpness on minimum cutting thickness and cutting surface integrity in ultra-precision machining. Journal of Material Processing Technology, 62, pp327-330, 1996.

[23] Shoichi Shimada, Naoya Ikawa, Toshio Sata. Brittle-Ductile Transition Phenomena in Microindentation and Micromachining. Annals of the CIRP vol.44/1, pp523-526, 1995.

[24] Zone-Ching Lin, Wun-Ling Lia, H.Y. Lin, C.R. Liu. Residual stress with different tool flank wear lengths in the ultra-precision machining of Ni-P alloys. Journal of Materials Processing Technology, 65, pp116-126, 1997.

[25] N.P. Hung, Z.W. Zang,K.K.Lee,C.F.Chai. Precision grinding and facing of copper- beryllium alloys. Precision Engineering, 23, pp293-304, 1999.

[26] Groover, Mikell. Fundamentals of Modern Manufacturing, Prentice Hall. Upper Saddle River, NJ (Now published by John Wiley & Sons, New York), 1996.

[27] Boothroyd, Geofferey and Winston A. Knight. Fundamentals of machining and machine tool. 2nd Edition, Marcel Dekker, New York, 1989.

[28] Chang-Xue(Jack) Feng. An experimental study of the impact of turning parameters on surface roughness. Paper no.2036, Proceedings of the Industrial Engineering Research Conference, 2001.

[29] L. F. Spencer. Electroless Nickel Plating- A Review. Metal Finishing, 72, 58, Dec.1974.

[30] Hitchiner M.P., Wilks J. Factors affecting chemical wear during machining, Wear,Vol-93,pp63-80, 1984.

[31] Moriwaki, T., Shamoto, E. Inoue, K. Ultraprecision Ductile cutting of Glass by applying Ultrasonic Vibration, Annals of CIRP,41(1),pp141-144, 1992.

[32] Glenn O. Mallory, Juan B, Hajdu. Electroless plating : fundamentals and applications. Chapter-4, sponsored and published by American Electroplaters and Surface Finishers Society, 1990.

[33] Hitchiner M.P., Wilks J. Factors affecting chemical wear during machining, Wear,Vol-93,pp63-80, 1984.

[34] R. Wada, H. Kodama, K. Nakamura. Wear characteristics of single crystal diamond tool, Annals of CIRP vol.29/1/, p47-52, 1980.

[35] John Wilks, Eileen Wilks, “Properties and Applications of Diamond” Chapter 13, Oxford, Butterworth and Heinemann, 1991.